2019

Morphological and morphometric analysis of Nekemias arborea and Ampelopsis aconitifolia (Vitaceae)

Sally Rose Gray
University of Northern Iowa

MORPHOLOGICAL AND MORPHOMETRIC ANALYSIS OF *NEKEMIAS ARBOREA* AND *AMPELOPSIS ACONITIFOLIA* (Vitaceae)

An Abstract of a Thesis

Submitted

in Partial Fulfillment

of the Requirements for the Degree

Master of Science

Sally Rose Gray

University of Northern Iowa

May 2019

ABSTRACT

Leaf morphology in angiosperms is not constrained by the leaf's important function of providing energy through photosynthetic reactions. In just one family, Vitaceae, it is easy to observe among it's over 900 species, various leaf shapes and sizes even among closely related species as well as within individual species. Observation of these leaf forms within species can be used to determine, for example where a vine transitions from the juvenile state to the adult state as well as their relationship to the spatial and temporal patterning of inflorescence initiation. Analysis of two species within the Ampelopsis clade, one that retained ancestral leaf characters, *Nekemias arborea,* was compared with a species containing derived leaf characters, *Ampelopsis aconitifolia,* so that leaf shape relationships between members of the grape family could be assessed. Knowledge about the members of the Ampelopsis clade can help to reveal a better understanding of the development of the very important commercial species, *Vitis vinifera* (grape). Leaf development along the vines of each species was tracked to draw comparisons and divergences in leaf shape. Structures along the vine, such as tendrils and axillary buds, were also noted to establish a vine pattern and to help determine whether a correlation exists between these traits and leaf shape changes. Scanning electron microscopy was used to observe leaf initiation and shape elaboration from the shoot apical meristem. Landmarks on mature leaves were established using vein and dissection patterns and were statistically analyzed. Morphometric analysis using Elliptic Fourier Descriptors (EFD) was performed to establish relationships in leaf form between two species of within Vitaceae.

MORPHOLOGICAL AND MORPHOMETRIC ANALYSIS OF *NEKEMIAS ARBOREA* AND *AMPELOPSIS ACONITIFOLIA* (Vitaceae)

A Thesis

Submitted

in Partial Fulfillment

of the Requirements for the Degree

Master of Science

Sally Rose Gray

University of Northern Iowa

May 2019

This Study by: Sally Rose Gray

Entitled:

Morphological and Morphometric Analysis of *Nekemias arborea* and *Ampelopsis aconitifolia*

has been approved as meeting the theses requirement for the

Degree of Master of Science

_____	_____
Date	Dr. Julie Kang, Chair, Thesis Committee
_____	_____
Date	Dr. Steve L. O'Kane Jr., Thesis Committee Member
_____	_____
Date	Dr. Tilahun Abebe, Thesis Committee Member
_____	_____
Date	Dr. Jennifer Waldron, Dean, Graduate College

ACKNOWLEDGEMENTS

First and foremost I would like to thank Dr. Julie Kang for her patience, wisdom, and guidance throughout the research and writing processes. From her I have gained valuable skills that will help me in all future endeavors. None of the following work would have been possible without her. I would also like to thank Dr. Steve O'Kane and Dr. Tilahun Abebe for agreeing to serve on my thesis committee and providing insight and support on this project. Additionally, Dr. Kenneth Elgersma and his vast knowledge of statistical methods was vital to the data analysis process and provided me with a smoother road on this journey than would otherwise have been possible. The previous research of Dr. Daniel Chitwood and Dr. Jean Gerrath was extremely important to the methodology and data analysis within this study.

I would also like to express my appreciation for the United States Department of Agriculture (USDA) for providing the plants necessary for analysis. Space and equipment supplied by the University of Northern Iowa Botanical Center and Biology Department allowed me the scientific freedom to explore different avenues of analysis because of the variety of tools available to me. Finally, I am grateful to the College of Humanities, Arts and Sciences (CHAS) for the funding they have awarded to me for this research through the Summer Undergraduate Research Program (SURP) and the Graduate Research Awards for Student Projects (GRASP). These people and departments are just as responsible for the products of this research as I am.

TABLE OF CONTENTS

LIST OF FIGURES

CHAPTER 1

INTRODUCTION

Due to the importance of the leaf to a plant's survival, variation among leaf morphologies in the angiosperms is important to consider. Leaves evolved independently in two groups of vascular plants, the lycophytes and the euphyllophytes, which diverged 400 million years ago (Floyd and Bowman 2006). There are many genetic and environmental factors that play a role in the emergence of the many leaf forms that occur both within and among species or within genera. For instance, shade produced by the leaves of competitor plants, can induce a shade-avoidance response of leaf enlargement and elongation in wild tomato plant leaves. This foliar shade response was shown to alter the efficiency of water use and the plant's response to shade (Chitwood et al. 2012).

The shoot apical meristem (SAM) is a dome-shaped region of undifferentiated cells located at the tip of a shoot or vine. The *KNOTTED1-like HOMEOBOX (KNOX1)* gene is expressed in the SAM to keep cells in an indeterminate state so that the plant always retains a collection of stem cells for wound response and continual growth or maintenance of new organs (Kim et al. 2003). When a leaf is initiated in the SAM, *KNOX1* is downregulated in the incipient leaf primordia on a lateral region of the SAM so that cells can become determinate and begin to form the leaf primordia (Lincoln et al. 1996; Uchida et al. 2009; Hay and Tsiantis 2010). As the leaf primordium grows, presence or absence of *KNOX1* expression within regions of the leaf determines leaf shape. Typically, in simple-leaved plants, *KNOX1* is downregulated in the primordium resulting in a leaf with a single blade (Uchida et al. 2009). In plants with compound

leaves such as *Cardamine hirsuta* and tomato, after initiation from the SAM, the leaf primordium regains *KNOX1* activity in specific locations along the leaf margin, resulting in regions of prolonged *KNOX1* activity (Hay and Tsiantis 2006; Müller et al. 2006; Barkoulas et al. 2008). These regions, with active cell division, then become outgrowths on the developing leaf, later accounting for the leaflets that are present in compound leaves (Hagemann and Gleissberg 1996). The variability in where, when, and how *KNOX1* is expressed, along with activity of other genes, plays a key role in the accumulation of the many leaf forms observed today (Hay and Tsiantis 2006).

The Vitaceae (the grape family) is a widely-distributed, agriculturally important group of plants composed of over 900 species and 15 genera, including *Vitis,* which produce commercial table grapes, juice, and wine (Wen et al. 2014). This family is morphologically diverse, with traits that include a range of varying leaf shapes from simple to compound (Jones et al. 2013). While research is focused predominantly on commercial grapes, there has been an abundance of research studying the phylogenetic relationship of the species within the Vitaceae (Jansen et al. 2006; Soejima and Wen 2006; Lu et al. 2013; Wen et al. 2014; Gerrath et al. 2015; Wen et al. 2018). These studies have furthered our understanding of the relationship of species that have retained ancestral characters, which includes *Nekemias arborea*, and their relationship to those containing derived traits, such as *Ampelopsis aconitifolia.*

The *Ampelopsis* clade is composed of the North I, North II, and South groups which were organized and categorized by Nie et al. (2012) (Figure 1). Members of the South group are native to Australia, Africa, and South America. Both of the Northern

groups are comprised of the *Ampelopsis* genus. Based on previous floral analyses, the *Ampelopsis* and *Nekemias* genera are considered most similar to the ancestral form, with *Vitis* containing the most derived characters, and *Ampelocissus* being intermediate between the two genera (Ingrouille et al. 2002). The earliest fossil records for the *Ampelopsis* clade, dating back to the Paleocene, have been found in North America, implying that this is where the common ancestor to the clade lived. The North I group contains only leaves that are pinnately or bipinnately compound and is categorized as part of the *Leeaceifoliae* section of the *Ampelopsis* clade (Lacroix et al. 1990). *Nekemias arborea* is a member of this group and has many similar characters to *Leeaceae*, the most closely related family to *Vitaceae* (Figure 1) (Nie et al. 2012). Characters shared between *Leea* and *Nekemias* could offer a window into the morphology of their most recent common ancestor.

North I plants can be found in North America and Eastern Asia. North II is the *Ampelopsis* section of the clade whose plants contain leaves that are simple, palmately-divided, or palmately-compound. North II plants are native to North America, central Asia, Eastern Asia, and Europe. *Ampelopsis aconitifolia* is a member of the North II group where leaf forms include simple, palmately-lobed, and palmately-compound. This group could serve as an interesting research subject to reveal the transition from ancestral compound forms back to a less complex morphology (Nie et al. 2012) (Figure 1).

Ampelopsis is one of 15 recognized genera in the Vitaceae and contains about 25 species (Soejima and Wen 2006). *Ampelopsis* was previously considered to be paraphyletic, but has recently been divided into two genera based on nuclear data, leaf

morphology, and axillary bud analysis (Wen et al. 2018). *Ampelopsis* is described as having simple, trifoliate, or palmately compound leaves. The newly distinguished genus, *Nekemias* (previously *Ampelopsis*), has been described as having pinnately compound leaves and complex axillary buds (Wen et al. 2014). Analyzing the leaves as well as structural patterns along the vine within the genus, which is considered to maintain the most ancestral characters (*Ampelopsis*), and comparing them to its hypothesized next-closest relative can provide insights into the evolution of the grape family.

Leaf form in the Vitaceae has been vigorously studied in the past decades to unravel the history of leaf evolution in the family. From genetic analyses, it has been hypothesized that the most recent common ancestor of all of its members had compound leaves, like *Leea*, the sister group to Vitaceae (Lu et al. 2013). This was determined from the expression pattern of the *KNOX1* gene in the development of both simple and compound leaves (Müller et al. 2006; Champagne et al. 2007; Uchida et al. 2009). While the presence of *KNOX1* activity during compound leaf development is not unusual, the presence of *KNOX1* activity in the developing leaf primordia of simple leaves (Bharathan 2002) implies that simple leaves are a derived character within this family. Analysis of conserved and derived traits between the leaf forms of different members of Vitaceae can aid in the support of phylogenetic trees that are being constructed (Lu et al. 2013).

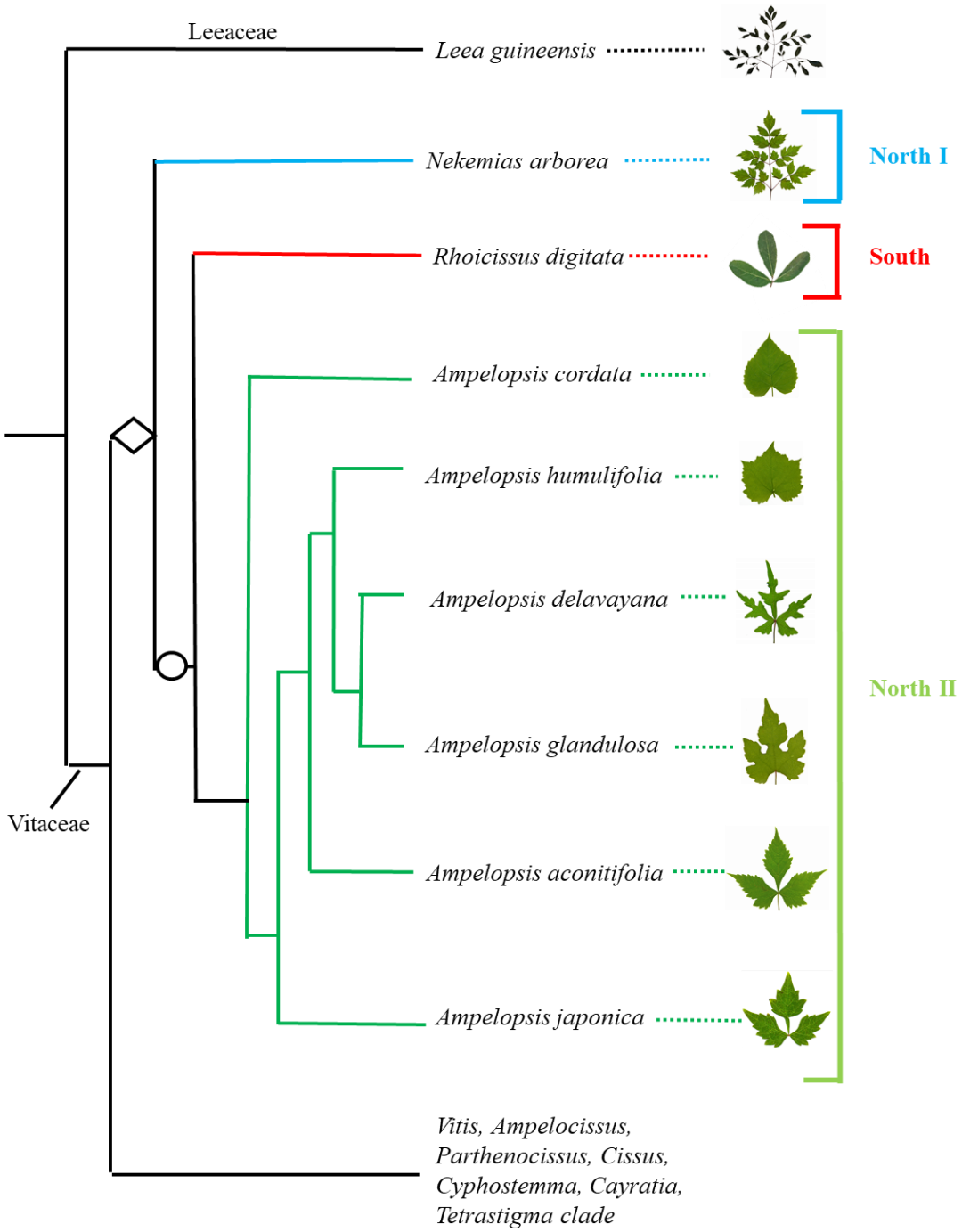

Figure 1: Vitaceae family phylogeny**.** Most recent phylogenetic tree adapted from a consensus tree by Nie et al. 2012 based on a maximum clade credibility tree. The node with the diamond represents the common ancestor to the Ampelopsis clade. The branch with the circle represents the only branch with a bootstrap value lower than 0.93, the value being 0.71. Leaf shape examples of each species are shown to the right.

Ampelography is the science of characterizing vine species and cultivars used for winegrowing, rootstock collection, clonal collection, table-grape collection, and more (Dexheimer 2011). It was developed in France in the late 19th century during the Phylloxera crisis (Chitwood et al. 2014). This crisis was caused by aphids carried across the ocean from North America to Europe on vines used for experimental and grafting purposes (Tassie 2010). After French scientists discovered that the aphids had travelled from North America, growers suggested grafting *Vitis vinifera* vines together with the resistant American line (Banerjee et al. 2010). The method was tested in Texas and found to be a success, saving the French wine industry and showing that ampelography, studying these plant species and their characteristics, can help to address diseases or other problems that need to be solved in the future. There is both molecular and morphological ampelography, the former is useful for problem solving in the lab, and the latter is useful for identification purposes in the field (Schneider 1996; Chitwood et al. 2014).

One use of ampelography is to analyze heteroblasty, which refers to the gradual change in leaf form along a vine or plant as it matures (Calonje et al. 2004). This method aids in identification of plants and is helpful in establishing relationships between species within a genus, as different members of a genus may exhibit different shoot patterns (Costa et al. 2012). The woody, climbing plants of Vitaceae have five previously established, specific patterns of tendril and axillary bud growth along their vines (Gerrath et al. 2001; Gerrath et al. 2004). The presence of tendrils, which are not found in the sister family, Leeaceae, may also aid in the identification of the transition to the adult phase along the vine, as they are a sign of reproductive maturity (Gerrath et al. 2015).

Tendrils along the woody vines of Vitaceae give them access to light in the upper canopy of dense, forested areas by attaching to surrounding structures and allowing the plant to grow vertically (Lu et al. 2013; Sousa-Baena et al. 2018). Production of tendrils requires much less energy than synthesis of woody material in cell walls along the entire vine (Jaffe and Galston 1968). However, this is not the only function of the tendril in the grape family. Tendrils of many plant species are modified leaves, shoots, or stipules, such as those of Fabaceae, Cucurbitaceae, and Smilacaceae (Zhang et al. 2015). Tendrils of Vitaceae are not homologous to those structures, instead they are homologous to the inflorescence (Díaz-Riquelme et al. 2014). This was shown through detection, in tendrils and inflorescences but not leaves, of *VASCULAR ADHESION PROTEIN 1* (*VAP1*) expression in *Vitis vinifera* and its *APETELA1* (*AP1*) ortholog in five other *Vitaceae* species representative of their clades (Zhang et al. 2015). Through this and various other genetic studies, it has been shown that tendrils are homologous among members of the grape family (Srinivasan and Mullins 1978). This information about gene expression in tendrils is important because general tendril formation patterns can be signs of the maturity of the vine and may be correlated with the maturity of leaf form (Gerrath et al. 2015).

The hypothesis about the correlation of mature leaf form and tendril formation is supported by the knowledge that hormones involved in the initiation and formation of tendrils are also involved in the formation of leaf shape (Maksymowych and Maksymowych 1973; Murray et al. 2012). Studies on *Vitis vinifera* have shown that tendrils contain gibberellic acid (GA) to avoid their transition into the inflorescence stage

and only the presence of cytokinins later on allow the tendrils to progress to the inflorescence stage (Srinivasan and Mullins 1978; Díaz-Riquelme et al. 2014). Noting the location of initiation of the first tendril may give insight into reasons behind leaf shape changes along the vine.

Analysis of the changes in leaf form along a vine is another way of observing derived and conserved characters. When observing a vine, first-formed leaves reside closer to the base of the plant than more recently initiated leaves (Mueller 1982). The older leaves that arise when the plant is younger, do not exhibit the adult leaf form (Bongard-Pierce et al. 1996). In fact, the first couple of leaves to arise out of a growing vine are the product of a still-juvenile vine and therefore do not exhibit the known adult leaf form (Jones 1999). Generally, the juvenile leaves are simple in shape. It is not until more distal nodes are reached that the leaves reach true adult form which is generally more complex than juvenile leaves (Zotz et al. 2011; Poethig 2013). By examining how these leaves change along the vine, it is possible to improve identification methods and establish a pattern for leaf change across different members of the grape family (Plotze et al. 2005).

One way of analyzing leaf form is through establishment of morphological landmarks (Zotz et al. 2011; Poethig 2013; Migicovsky et al. 2015; Chitwood et al. 2016; Klein et al. 2017). Landmarks are points and measurements taken between them provide a description of the object being evaluated (Park et al. 2013). When performing a statistical analysis of shape using landmarks, it is important to establish landmarks that will best represent the distinct features of the leaf that may be subject to change (Costa et

al. 2012). In leaves, these features might be overall leaf length, vein length, and angle between leaflets. By comparing these measurements along the vine as well as across species and combining them with the overall shape patterns obtained from morphometric analysis, patterns of heteroblasty can be established (Galet 1952; Chitwood et al. 2014).

Until recently, examination of leaf shape in the form of a morphometric analysis was an extremely time-consuming and subjective task. Determining which measurements are most important to collect as well as accurately comparing leaf forms can lead to differing results between studies based on what the researcher deems important and how the researcher goes about comparing leaf forms (Remagnino et al. 2017). A tool that has made this process much easier and more accurate is geometric morphometric analysis (Adams et al. 2004; Chitwood and Otoni 2017; Klein et al. 2017; Migicovsky et al. 2018). By using the SHAPE program, overall leaf shape of each species can be numerically recorded and compared to establish similarities and differences in form (Iwata and Ukai 2002; Chitwood et al. 2015). Applying a numeric value to the morphology of each leaf assures that every leaf margin is being described using the same method, removing human error and subjectivity from the process.

This thesis will focus on the developmental morphology and morphometric analysis of *Nekemias arborea* and *Ampelopsis aconitifolia* leaf shape. It is expected that results will support the prediction that the common ancestor of Vitaceae had compound leaves. *Nekemias arborea* is the only species that has bipinnately compound leaves in this family. By studying a member of the Vitaceae with the ancestral character of compound leaves and comparing it with a species containing a derived leaf form, as well

as to previously studied species in the family (Jones et al. 2013), the goal of this research is to help further understand derived characteristics and reveal developmental traits of the common ancestor. Thus, new information from this study will help uncover more about the evolutionary history of the Vitaceae. In addition, grape fruit yield, fruit quality, plant upkeep, and disease resistance will be enhanced by a greater knowledge of all members of Vitaceae.

CHAPTER 2

MATERIALS AND METHODS

Seed Germination and Plant Care

Seeds of *Nekemias arborea* were obtained from the United States Department of Agriculture (USDA) at Iowa State University (Ames, Iowa, USA) germplasm collection (accession PI 656799). To begin germination, seeds were placed in 14 mL FALCON polypropylene round bottom tubes (Fisher Scientific, Pittsburgh, PA). The tubes were filled with 10 mL of distilled water and left for 24 hours with the cap loose. The water was then removed and 5 mL of 1.5% H_2O_2 (hydrogen peroxide) was added for chemical scarification and left for 24 hours with the cap tight. Once the H_2O_2 was removed, the seeds were rinsed in distilled water and blotted dry. Double the seeds' volume of a 1000 ppm solution of gibberellic acid (GA) (PhytoTechnology Laboratories, Lenexa, KS) was added to the tubes for 24 hours at room temperature with the cap tight for an airlock. The gibberellic acid (GA) was then rinsed off with distilled water and the seeds were blotted dry and stored for 21 days on moistened blotting paper at 2-4^{o}C.

Once the 21-day chilling period concluded, seeds were rinsed with distilled water and once again soaked in double their volume of gibberellic acid (GA) for 24 hours. Finally, seeds were planted in small-compartment seed trays (Hummert International, 4500 Earth City Expy, Missouri, USA) and placed under a grow-light during a 16-hour day: 8-hour night cycle. After the seeds germinated (approximately 20 days after planting) and the cotyledons were fully grown and uncurled, seedlings were transplanted into 2.25-inch pots (Hummert International, Earth City, MO) and placed in

research greenhouses at the University of Northern Iowa Botanical Center under shade cloth.

Dormant *Ampelopsis aconitifolia* plants were obtained from Dancing Oaks Nursery (Monmouth, OR), repotted in one-gallon pots (Hummert International, Earth City, MO) and placed in research greenhouses. All plants were observed and watered daily. They were fertilized biweekly with Jack's Professional 20-20-20 General Purpose fertilizer (Fosters Incorporated, Waterloo, IA).

Leaf Collection and Image Processing

In order to facilitate the leaf collection process, the nodes of vines of each species were labeled with tape to keep track of what node each leaf initiated from. Vines of twelve *A. aconitifolia* plants and three *N. arborea* plants were monitored. Leaves were measured weekly to ensure that collection did not interrupt the growth process. Once it was determined that the leaf had reached its maturity (approximately 42 days after initiation), it was cut from the vine, the node it was found at was recorded, and photographed using a Nikon Coolpix L110 Digital 12.1 MP digital camera (Nikon Incorporated, Melville, NY) with a ruler for scale.

Leaf pictures were processed using Adobe Photoshop CC 2017 (Adobe, San Jose, CA) to prepare them for the ImageJ 1.46r (National Institutes of Health, Bethesda, MD) and SHAPE 1.3 (National Agricultural Research Organization, Ibaraki, JP) programs. To be prepped for ImageJ, leaf backgrounds were removed, leaves were placed on a solid white background, and saved as a JPEG. To prepare for the SHAPE program, leaves were filled in with black, placed on a white background, and saved as a Bitmap.

IMAGEJ

Landmarks (Figure 2) were determined for each species and leaf measurements were taken using ImageJ software. Selected angles and vein lengths as well as area and perimeter of the leaf were measured and data was saved in a comma-separated value file for further statistical analysis in R.

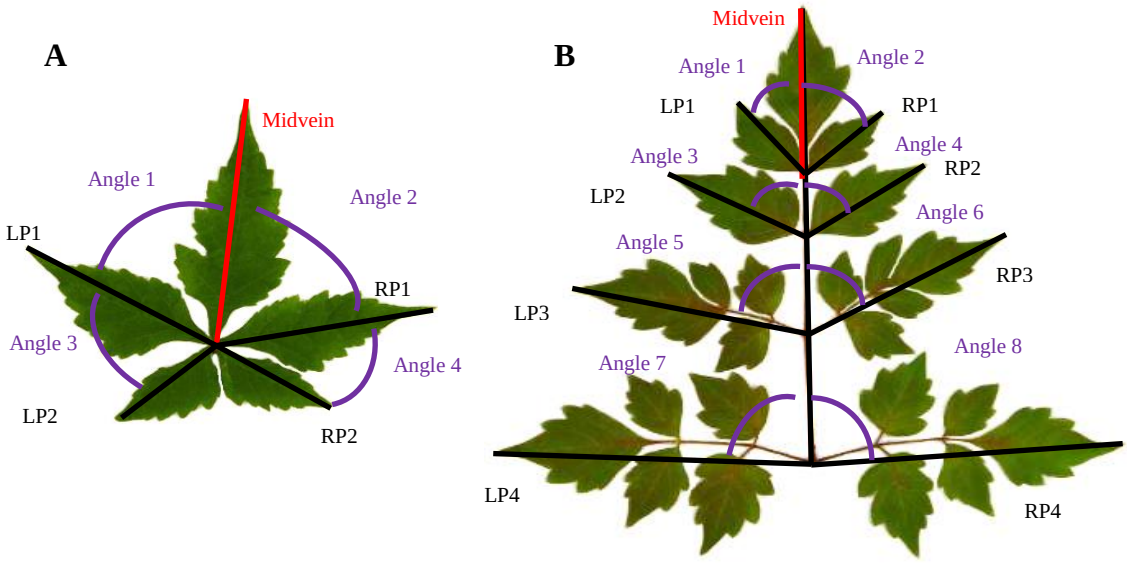

Figure 2: Mature leaves of *N. arborea* and A. *aconitifolia*. (A) A representative mature *A. aconitifolia* leaf labeled with all measurements taken. (B) A representative mature *N. arborea* leaf labeled with all measurements taken. LP1 = left primary leaflet 1; LP2 = left primary leaflet 2; LP3 = left primary leaflet 3; LP4 = left primary leaflet 4; RP1 = right primary leaflet 1; RP2 = right primary leaflet 2; RP3 = right primary leaflet 3; RP4 = right

Morphometric Analysis

Morphometrics were completed using the SHAPE program (Iwata and Ukai 2002). The first step of using the program was to translate all black and white bitmap images of the leaves into chain codes. Chain coding is a translation of the leaf's shape into a numeric description of that shape (Iwata and Ukai 2002). To begin chain coding, one point on the leaf margin was selected and, using a clock-like wheel of numbers, a code was created to describe the outline of the leaf. Chain codes were then used to calculate normalized Elliptic Fourier Descriptors (EFD) (Kuhl and Giardina 1982), which were processed using principal component analysis (PCA) to obtain the shape variation of the leaves (Iwata and Ukai 2002).

Elliptic Fourier Descriptors quantify the chain code as a harmonic series (Migicovsky et al. 2018). The harmonic series is a sum of chain codes that allows leaf shapes at a node to be compared through PCA (Chitwood and Otoni 2017). This process includes orthogonally transforming the data in the harmonic series into linear principal components, which can then be viewed and compared to draw conclusions about any pattern in leaf form (Roberts and Everson 2001).

Statistical Analysis

Statistical analysis was conducted using R version 3.5.1 (R-Project, Vienna, AT), a command-line system for statistical analysis. Leaf measurement data obtained from ImageJ was entered into the program to construct of box plots and scatterplots. The data set from each measurement was analyzed separately to determine which model best fit the data. First, Akaike Information Criterion (AIC) scores were calculated using R to

locate which order polynomial regression to use (Appendix D, Figure D1-D2). AIC analysis applies a score of how each model fits the data, penalizing increases in complexity (Forster and Sober 2011). When analyzing data, the simplest model that represents the data should be selected, therefore the model that received the lowest AIC score was selected (Hall 2013).

After a specific model was selected for each variable, a one-way ANOVA was used to evaluate the variance between leaf measurements at each node along the vine. The model for this analysis is:

$$Y_{i,j,k} \sim N(\mu_{vine[i,j]} + X*\beta_{node} + X^2*\beta_{quadratic} + X^3*\beta_{cubic}, \sigma_{error})$$

$$\mu_{vine[i,j]} \sim N(\mu_{plant[i]}, \sigma_{vine})$$

$$\mu_{plant[i]} \sim N(\mu_{grand}, \sigma_{plant})$$

There are three levels to this model because the data analyzed was nested. For example, node number was nested within vine number which was nested within plant number because there is a connection between plant, vine, and that should be accounted for in the analysis. To adjust for this connection, the full formula for the model in the first line has two constraints listed below it. The tilda (~) indicates the distribution and N signifies a normal distribution with mean μ and standard deviation σ. Therefore, $Y \sim N(\mu, \sigma)$ can be read as the data following a normal distribution with a mean of μ and standard deviation of σ. The first line of the model contains the fixed effects of the node, such as the linear, quadratic, and cubic terms. The [i] represents the plant number being considered, the [j] indicates the vine number being considered, and the [k] lists which variable is being analyzed. If, for example, area is being analyzed, the model can be read as leaf area is

normally distributed around the mean of vine [j] on plant [i] adjusted to a third order polynomial regression with standard deviation σ. The second line adds to that formula the fact that there is variation from one vine to the next within a plant. The third line introduces that each plant has its own value which is normally distributed around a grand mean. The hierarchical model says that the means are normally distributed as well. Presence or absence of statistically significant variation was determined from an ANOVA based on this model and boxplots and scatterplots were constructed to visualize trends. A p-value of less than 0.05 was considered statistically significant. Both boxplots and scatterplots are shown to allow visualization of data point distributions within a node (boxplot) as well as visualization of the pattern that exists across nodes through the addition of a regression line (scatterplot).

Scanning Electron Microscopy

Shoot apical meristems (SAM) were collected off of shoot tips from both *N. arborea* and *A. aconitifolia* mature plants, then stored in formalin (Fisher Scientific, Pittsburgh, PA) acetic acid (Fisher Scientific, Pittsburgh, PA) mixture (90 mL:5 mL:5mL of 70% ethanol:formalin:acetic acid) to fix the samples. The apices were dehydrated through an ethanol (EtOH) series, starting out with 70% EtOH, moving through 80%, 90%, 95%, and 100% EtOH. Once the samples were dehydrated, the older leaves surrounding the meristem were dissected out using an Olympus SZx7 dissecting microscope (Olympus Corporation, Center Valley, PA) until the meristem was completely visible.

Once dissected, tissue samples were dried using a Tousimis Samdri-795 critical point dryer (CPD) (Tousimis Incorporated, Rockville, MD) with CO_2, reaching a critical point of 31^{o}C and 1072 psi. After drying, the samples were checked once more under the dissecting scope to ensure that no further dissection was needed. Meristems were coated with gold using a 108 auto Cressington Sputter Coater (Ted Pella Incorporated, Redding, CA). A Tescan Vega 3 Scanning Electron Microscope (Tescan Incorporated, Warrendale, PA) was used to visualize the meristems at 20kV and Vega TC software (VEGA Incorporated, Cincinnati, OH) was used to capture images.

CHAPTER 3

RESULTS

Leaf Structures

For both species, variability in leaflet number and sub-leaflet number exists within and across nodes. *Nekemias arborea* adult leaves are composed of primary, secondary, and tertiary leaflets while *Ampelopsis aconitifolia*

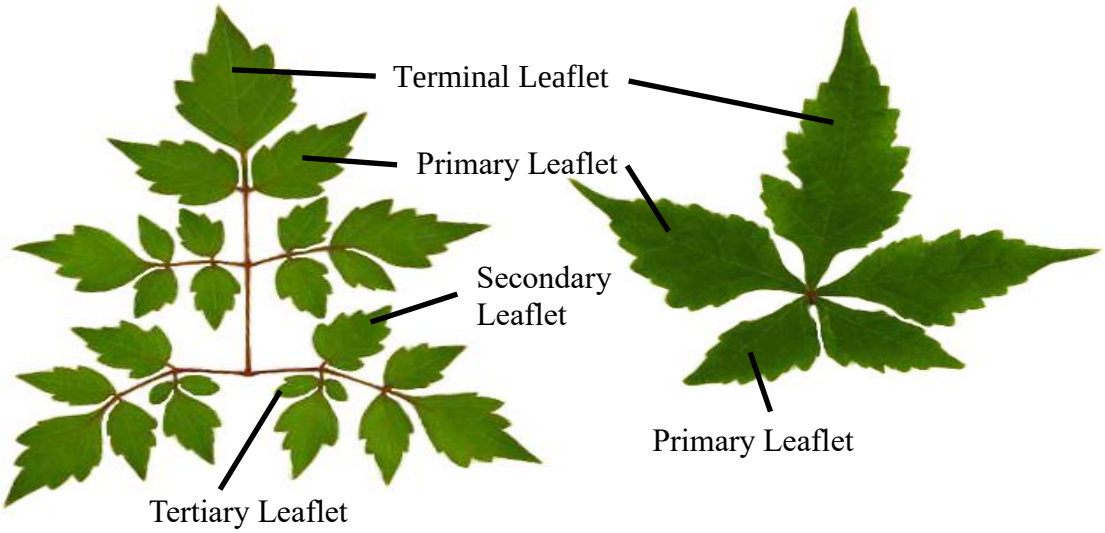

Figure 3: Mature leaves of each species. (A) A representative mature *N. arborea* leaf showing labeled primary, secondary, and tertiary leaflets. (B) A representative mature *A. aconitifolia* leaf showing labeled primary leaflets.

adult leaves are composed of only primary leaflets (Figure 3, A-B). Despite these differences, some patterns in form can be established. A table describing the leaf form at each node for each species is found in Appendix A, Figure A1. Mature adult leaves for every node were selected to represent the general leaf form at each respective position along the vine (Figure 4).

For *A. aconitifolia*, 64.1% of leaves found at node one were simple while the rest were trifoliate. Of the simple leaves, all had two serrations deeper than the others on the leaf margin between the midvein and each secondary vein (Figure 4A, leaf 1 asterisks). Of the trifoliate leaves, all leaflets were divided and attached at their base at the petiole. Nodes two through five were composed of all trifoliate leaves (Figure 4A, leaves 2-5). Serrations were more saw-toothed than the rounded serrations found at node one. The tips of the leaflets were sharply pointed rather than the rounded leaflet ends at node one (Figure 4A).

Of the leaves taken from node six, 94.1% were trifoliate. There was one leaf at this node that was pentafoliate. Of the trifoliate leaves, all contained two deep serrations on the two lateral leaflets between LP1 and LP2 (Figure 4A, leaf 6 arrowheads).

Nodes seven and eight were 64.7% and 92.3% trifoliate respectively, with deep serrations in secondary leaflets (Figure 4A, leaves 7-8). For the remaining leaves at these nodes, the two deep serrations extend all the way down to the petiole attachment, creating pentafoliate leaves. For nodes nine and ten, those full dissections into pentafoliate leaves are more consistent, resulting in 64.3% and 54.6% pentafoliate leaves, respectively (Figure 4A, leaves 9-10). This trend switches back to 75.0% trifoliate leaves at node eleven, with comparable or larger percentages at remaining nodes (Figure 4A, leaf 11). After node ten, no pentafoliate leaves occur but trifoliate leaves still contain deep serrations on the secondary leaflets (Figure 4A, leaf 11).

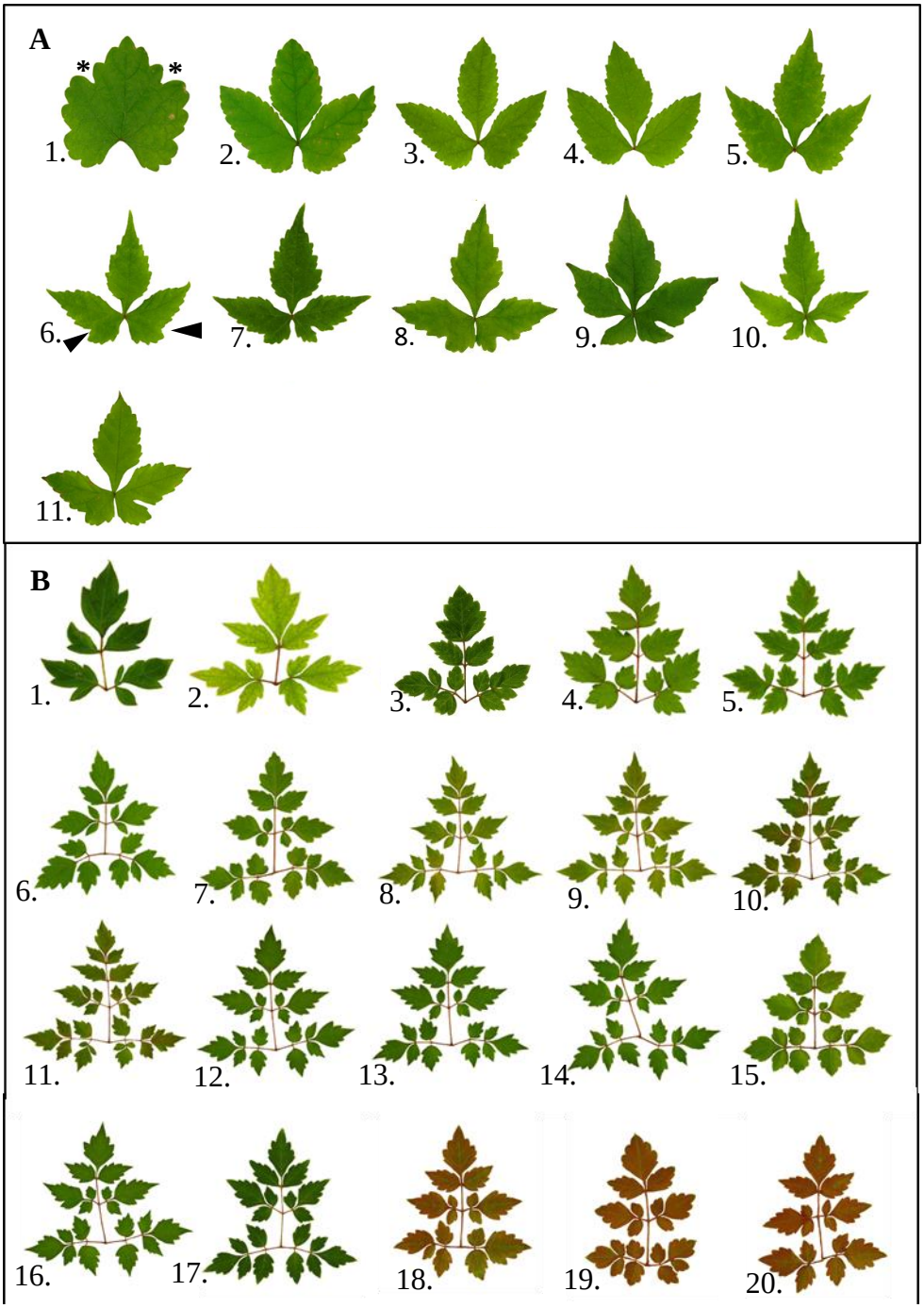

Figure 4: Representative leaf plates for each species. (A) Representative leaves from each node along the vine of *A. aconitifolia.* The (*) denotes the two deeper serrations than most found in all simple leaves of *A. aconitifolia.* Arrowheads denote the second set of deep serrations that develop around nodes six and seven. (B) Representative leaves from each node along the vine of *N. arborea.* For both plates, the number represents the node along the vine the leaf is from.

For *N. arborea,* leaves at the first node had one terminal primary leaflet and two pairs of lateral primary leaflets (Figure 4B, leaf 1). Serrations on these leaves were rounded. On all of these leaves, two secondary leaflets were present on the second pair of lateral primary leaflets (the set more proximal to the stem) (Figure 4B, leaf 1). 57.1% of leaves at both node two and node three were composed of the terminal primary leaf and the two pairs of lateral leaflets, just like those found at node one. The remaining leaves a third set of lateral leaflets present. On 42.9% of leaves found at node two and 71.5% of those found at node three, there were two pairs of secondary leaflets on the most proximal pair of primary leaflets.

Nodes four through seven were composed of 61.9% leaves with three pairs of leaflets and one terminal leaflet (Figure 4B, leaves 5-7). At these nodes, 42.9% of leaves had tertiary leaflets present on the pairs of lateral leaflets most proximal to the leaf's attachment to the stem (Figure 4B, leaves 5-7). Nodes eight through eleven contained 51.0% leaves with four pairs of leaflets, 33.3% of which had tertiary leaflets on the proximal pair of lateral leaflets (Figure 4B, leaves 8-11). At node eight, serrations have become more saw-toothed and more numerous (Figure 4B, leaf 8).

The trend of leaves at nodes twelve through twenty reverted back to that found at earlier nodes, with 84.2% of leaves having three pairs of lateral leaflets in addition to the terminal leaflet (Figure 4B, leaves 12-20). Of the leaves found at these nodes, just 22.2% had tertiary leaflets on the most proximal pair of lateral leaflets (Figure 4B, leaves 12-20). The last three to four leaves on each vine reverted back to the rounded, less numerous serrations found at the first seven nodes (Figure 4B, leaves 1-7, leaves 18-20).

SEM Analysis

Scanning electron microscope (SEM) images were collected and analyzed to assess leaf and leaflet initiation. In total, 86 *A. aconitifolia* meristems and 57 *N. arborea* meristems were collected from nodes where mature leaves form and imaged using the SEM. A table describing primordium characteristics within specific height ranges is shown in Appendix B.

The P1 (Primordia 1) stage of *A. aconitifolia* leaf development, show a small outgrowth from the SAM (Figure 5A). At the P2 stage, two small bulges, the precursors to the first pair of secondary leaflets, at each side of the primordium emerge (Figure 5B). The first pair of secondary leaflets are formed at the P3 stage of development (Figure 5C). The P4 stage shows a leaf that still has one pair of secondary leaflets but serrations have formed on the margins (Figure 5D). The P5 stage of leaf development shows that a second pair of secondary leaflets formed underneath the first pair (Figure 5E).

The six stages of early leaf development in *N. arborea* are shown in Figure 5 starting with P1 and ending with P6. The first stage, P1, of primordial leaf development consists of a small outgrowth of the SAM (Figure 6A). During the P2 stage of development, the first pair of lateral leaflets developed (Figure 6B). The second pair of lateral leaflets developed during the P3 stage (Figure 6C). At the P4 stage, the third pair of lateral leaflets developed (Figure 6D). Although the leaf still only has three pairs of lateral leaflets at the P5 stage, the beginning of the formation of secondary leaflets along the leaf margins have begun (Figure 6E). The P6 stage of development show more developed secondary leaflets and a fourth pair of lateral leaflets has emerged (Figure 6F).

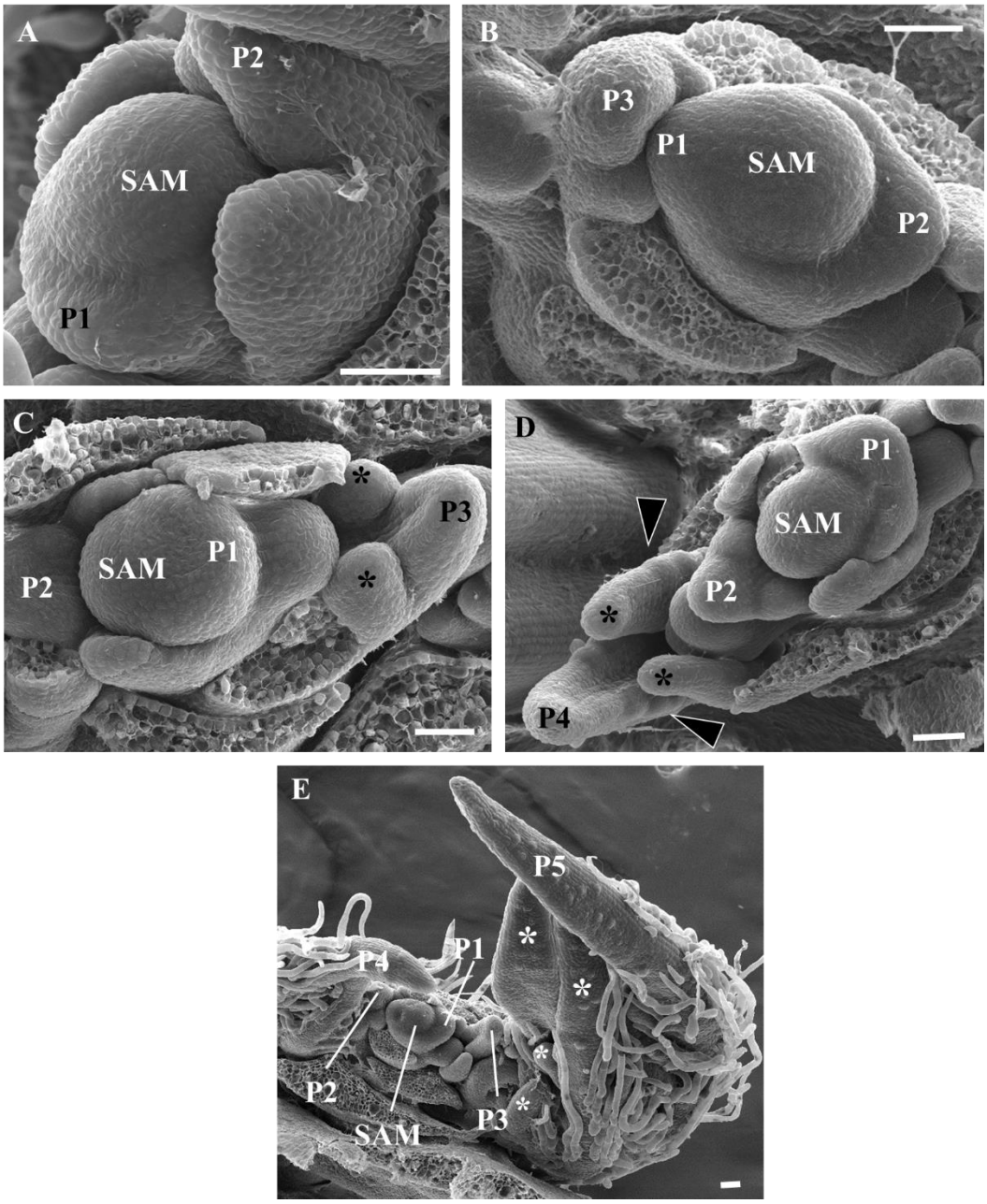

Figure 5: Scanning electron microscopy images (A-E) of the early developmental stages of *A. aconitifolia* leaves. Examples of stages P1-P5 are present on the pictures. All asterisks label the secondary leaflets. Arrowheads indicate serrations along the leaf margins. Scale bars = 50μm

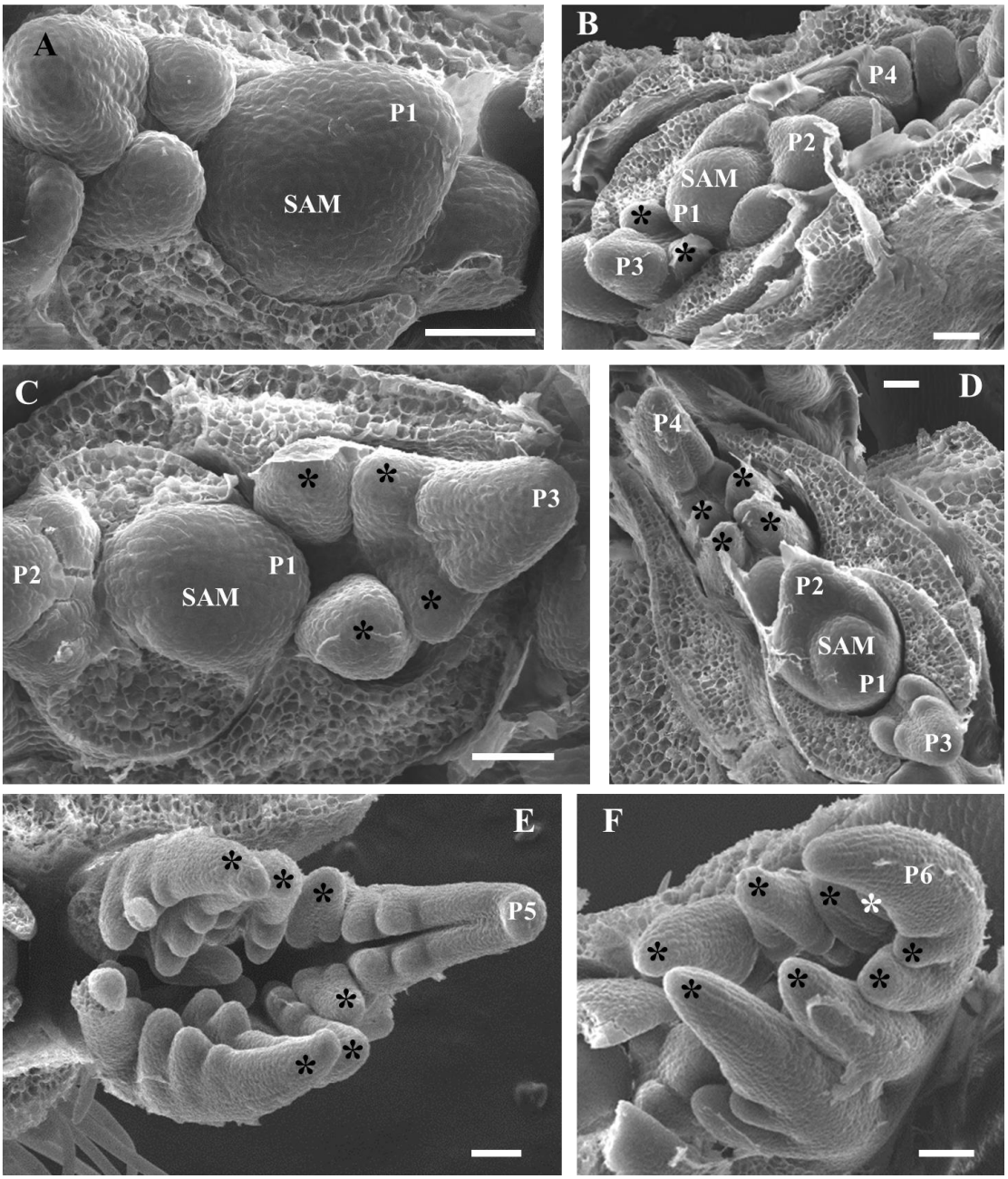

Figure 6: Scanning electron microscope images (A-F) of the six stages of early leaf development in *N. arborea.* Labels for P1-P6 can be found on the end of their respective leaf examples. All asterisks (*) mark the formation of lateral leaflets. Arrowheads point to the secondary leaflet precursors on the leaflet margins. Scale bars = 50μm

Leaf Morphometrics

In total, 150 *A. aconitifolia* leaves and 192 *N. arborea* leaves were analyzed for this study. On every leaf, several measurements were taken: area, perimeter, length of primary and secondary veins, and angles between primary and secondary veins (Figure 2A and B) and results were compiled, analyzed, and graphed using R.

For *A. aconitifolia*, eleven measurements were taken on each leaf: area, perimeter, midvein length, LP1 length, RP1 length, LP2 length, RP2 length, angle one, angle two, angle three, and angle four (see Figure 2A). For all measurements, the AIC scores showed that a third-order polynomial regression fits the data best.

For *N. arborea*, twenty measurements were taken on each leaf; area, perimeter, midvein length, total length, LP1 length, RP1 length, LP2 length, RP2 length, LP3 length, RP3 length, LP4 length, RP4 length, angle one, angle two, angle three, angle four, angle five, angle six, angle seven, and angle eight (see Figure 2B). For all measurements except for RP1, the AIC scores showed that a third-order polynomial regression fits the data best. The RP1 length showed that a second-order polynomial regression was more suitable.

Graphs were generated showing the trend of the area of *A. aconitifolia* and *N. arborea* leaves at each node (Figure 7). For *A.* aconitifolia, both the boxplot and the regression line on the scatterplot show that there is a steady increase in the average area which peaks at 60.7 cm^2 at node three, after which there is a gradual decrease in area as the node number increases (Figure 7B-C). For *N. arborea*, both the boxplot and the regression line on the scatterplot show that there is a steady increase in average area

which peaks at 63.0 cm^2 at node seven (Figure 7E-F). After node seven, there is a gradual decrease in area as the node number increases with a slight increase in area again near the last node (Figure 7E-F).

The trends in the perimeter of *A. aconitifolia* and *N. arborea* leaves at each node were analyzed (Figure 8). For *A. aconitifolia,* both the boxplot and the regression line on the scatterplot show that there is a steady increase in average perimeter which peaks at 60.3 cm at node four (Figure 8B-C). Afterward, there is a gradual decrease in perimeter as the node number increases (Figure 8B-C). The boxplot and the regression line on the scatterplot for *N. arborea* show that there is a steady increase in average perimeter which peaks at 162.0 cm at node eight (Figure 8E-F). There is a gradual decrease in perimeter after node eight as the node number increases with a slight increase in perimeter again near the last node (Figure 8E-F).

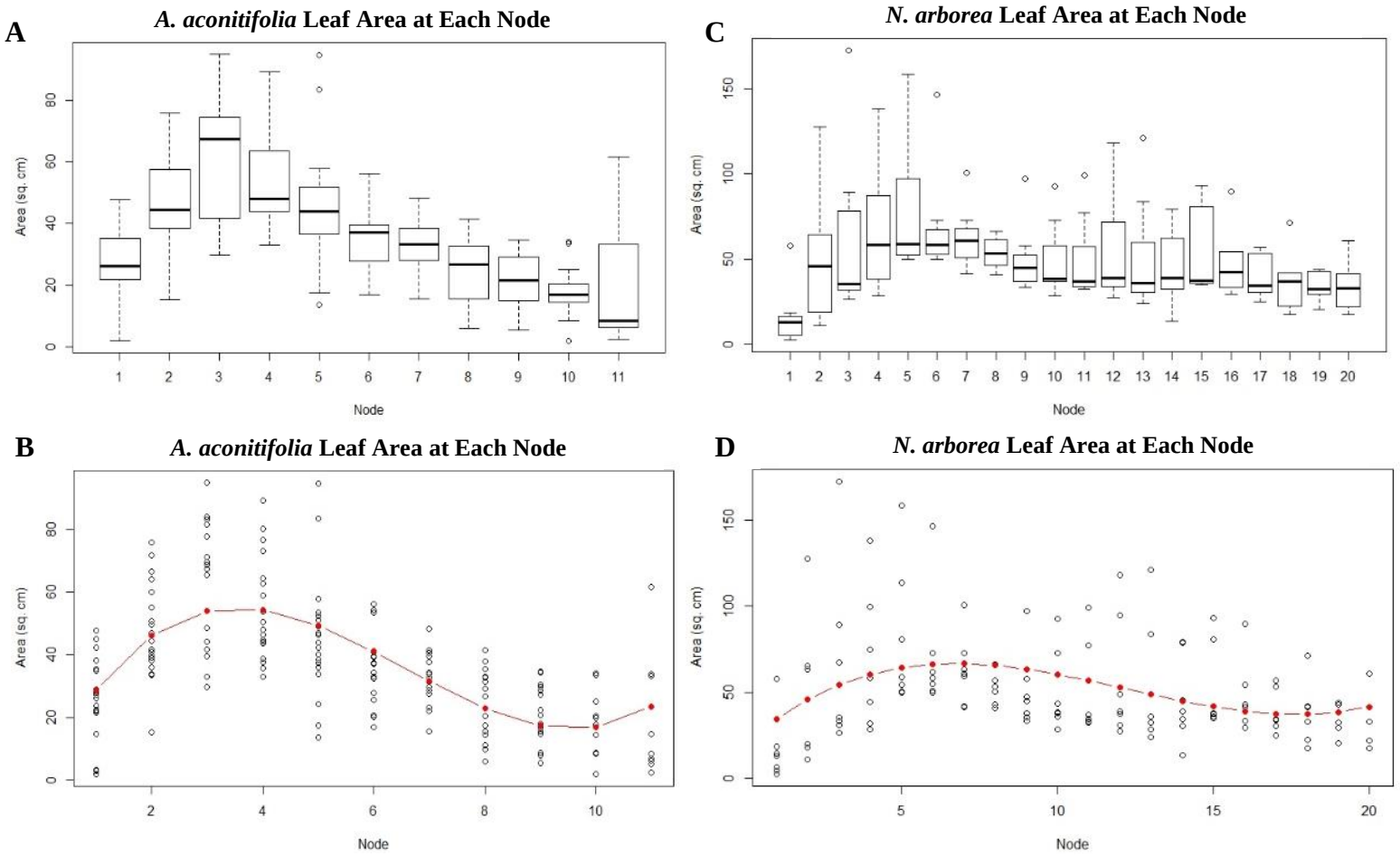

Figure 7: Leaf area at each node. (A) A boxplot showing the area measurements at each node along *A. aconitifolia* vines. (B) A scatterplot showing the area measurements at each node along *A. aconitifolia* vines with a regression line portraying the trend of the data shown in red ($p<0.0001$). (C) A boxplot showing the leaf area measurements at each node along *N. arborea* vines. (D) A scatterplot showing the leaf area measurement at each node along *N. arborea* vines with a regression line portraying the trend of the data shown in red ($p<0.0001$).

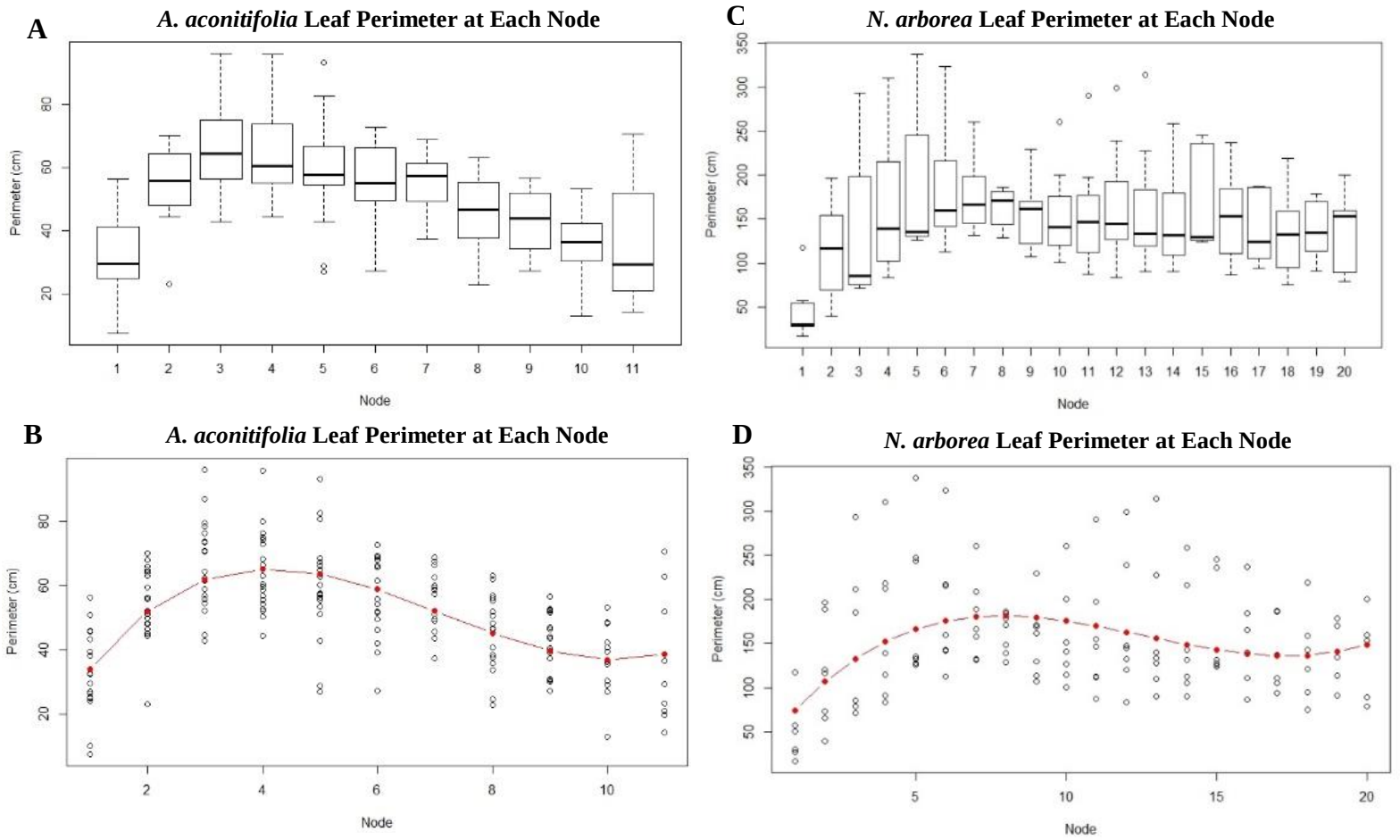

Figure 8: Leaf perimeter at each node. (A) A boxplot showing the perimeter measurements at each node along *A. aconitifolia* vines. (B) A scatterplot showing the perimeter measurements at each node along *A. aconitifolia* vines with a regression line portraying the trend of the data shown in red ($p<0.0001$). (C) A boxplot showing the leaf perimeter measurements at each node along *N. arborea* vines. (D) A scatterplot showing the leaf perimeter measurement at each node along *N. arborea* vines with a regression line portraying the trend of the data shown in red ($p<0.0001$).

The trend of the midvein length of *A. aconitifolia* and *N. arborea* leaves at each node were analyzed and graphed (Figure 9). Both the boxplot and the regression line on the scatterplot show that there is a steady increase in average midvein length which peaks at 8.8 cm at node four (Figure 9A-B) for *A. aconitifolia*. Next, there is a gradual decrease in midvein length as the node number increases (Figure 9A-B). For *N. arborea*, both the boxplot and the regression line on the scatterplot show that there is a steady increase in average length which peaks at 5.1 cm around node seven (Figure 9C-D). There is a gradual decrease in length after node eight as the node number increases with a slight increase in length again near the last node (Figure 9C-D).

LP1 length measurements of *A. aconitifolia* and *N. arborea* leaves at each node were analyzed and their trends were graphed (Figure 10). The boxplot and the regression line for *A. aconitifolia* on the scatterplot show that there is a steady increase in average length which peaks at 7.2 cm at node four followed by a gradual decrease in length more distally along the vine (Figure 10A-B). This same trend is exhibited along the vines of *N. arborea* with the peak occurring at a more distal node than that of *A. aconitifolia.* The node with the highest measurement of LP1 length for *N. arborea* is around node eight with an average value of 3.1 cm (Figure 10C-D).

Graphs were generated showing the trend of the RP1 length of *A. aconitifolia* and *N. arborea* leaves at each node (Figure 11). Similar to the trends of other measurements, the RP1 length for both species follows the same pattern of increasing gradually, peaking at a certain node, and then gradually decreasing (Figure 11A-D). For *A. aconitifolia,* this

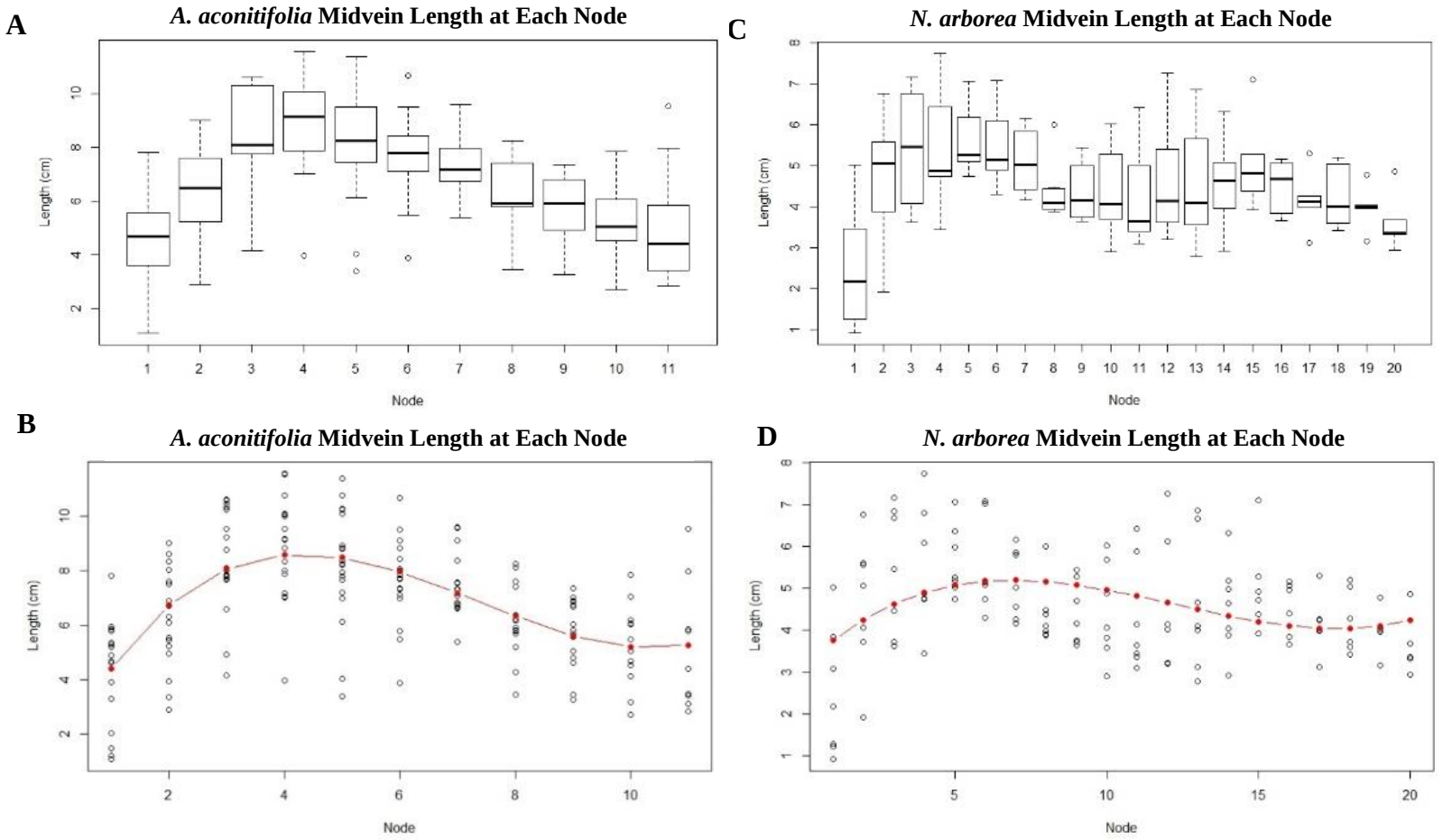

Figure 9: Leaf midvein length at each node. (A) A boxplot showing the midvein length in centimeters at each node along *A. aconitifolia* vines. (B) A scatterplot showing the midvein length in centimeters at each node along *A. aconitifolia* vines with a regression line portraying the trend of the data shown in red ($p<0.0001$). (C) A boxplot showing the midvein length in centimeters at each node along *N. arborea* vines. (D) A scatterplot of the midvein length in centimeters at each node along *N. arborea* vines with a regression line portraying the trend of the data shown in red ($p<0.0001$).

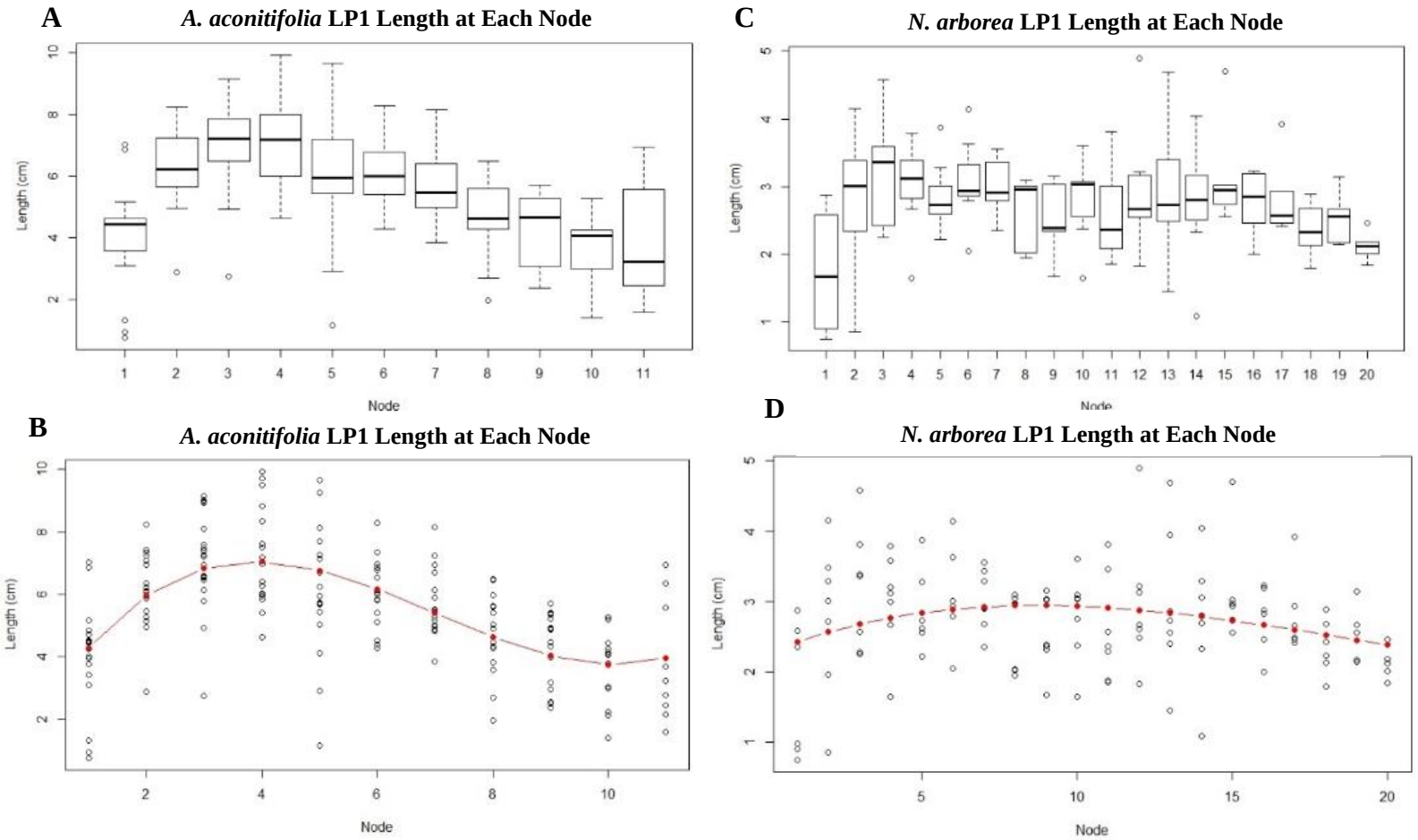

Figure 10: LP1 length at each node. (A) A boxplot showing LP1 length in centimeters at each node along *A. aconitifolia* vines. (B) A scatterplot showing LP1 length in centimeters at each node along *A. aconitifolia* vines with a regression line portraying the trend of the data shown in red ($p<0.0001$). (C) A boxplot showing LP1 length in centimeters at each node along *N. arborea* vines. (D) A scatterplot showing LP1 length in centimeters at each node along *N. arborea* vines with a regression line portraying the trend of the data shown in red ($p=0.0241$).

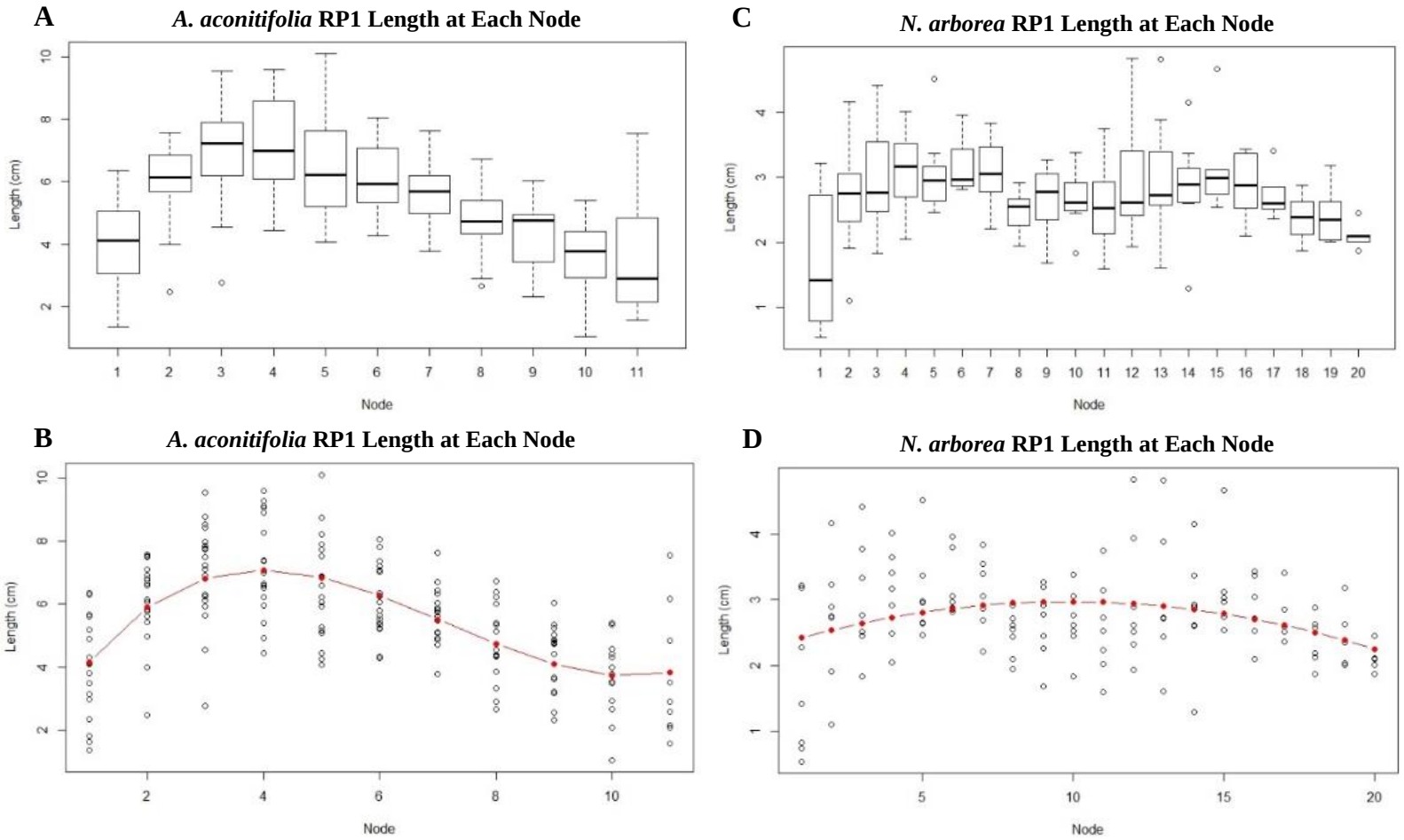

Figure 11: RP1 length at each node. (A) A boxplot showing RP1 length in centimeters at each node along *A. aconitifolia* vines. (B) A scatterplot showing RP1 length in centimeters at each node along *A. aconitifolia* vines with a regression line portraying the trend of the data shown in red ($p<0.0001$). (C) A boxplot showing RP1 length in centimeters at each node along *N. arborea* vines. (D) A scatterplot showing RP1 length in centimeters at each node along *N. arborea* vines with a regression line portraying the trend of the data shown in red ($p=0.0013$).

peak occurs at nodes three and four with an average of 1.2 cm (Figure 11A-B) and for *N. arborea*, the peak occurs at node seven with an average of 3.1 cm (Figure 11A-D).

Similarly, the average LP2 length of *A. aconitifolia* leaves peaked at node three with a value of 3.9 cm (Figure 12A-B). *N. arborea* LP2 leaf measurements peaked around node six with an average value of 5.1 cm (Figure 12C-D). Both species show the trend of lengths decreasing in value gradually after that peak (Figure 12).

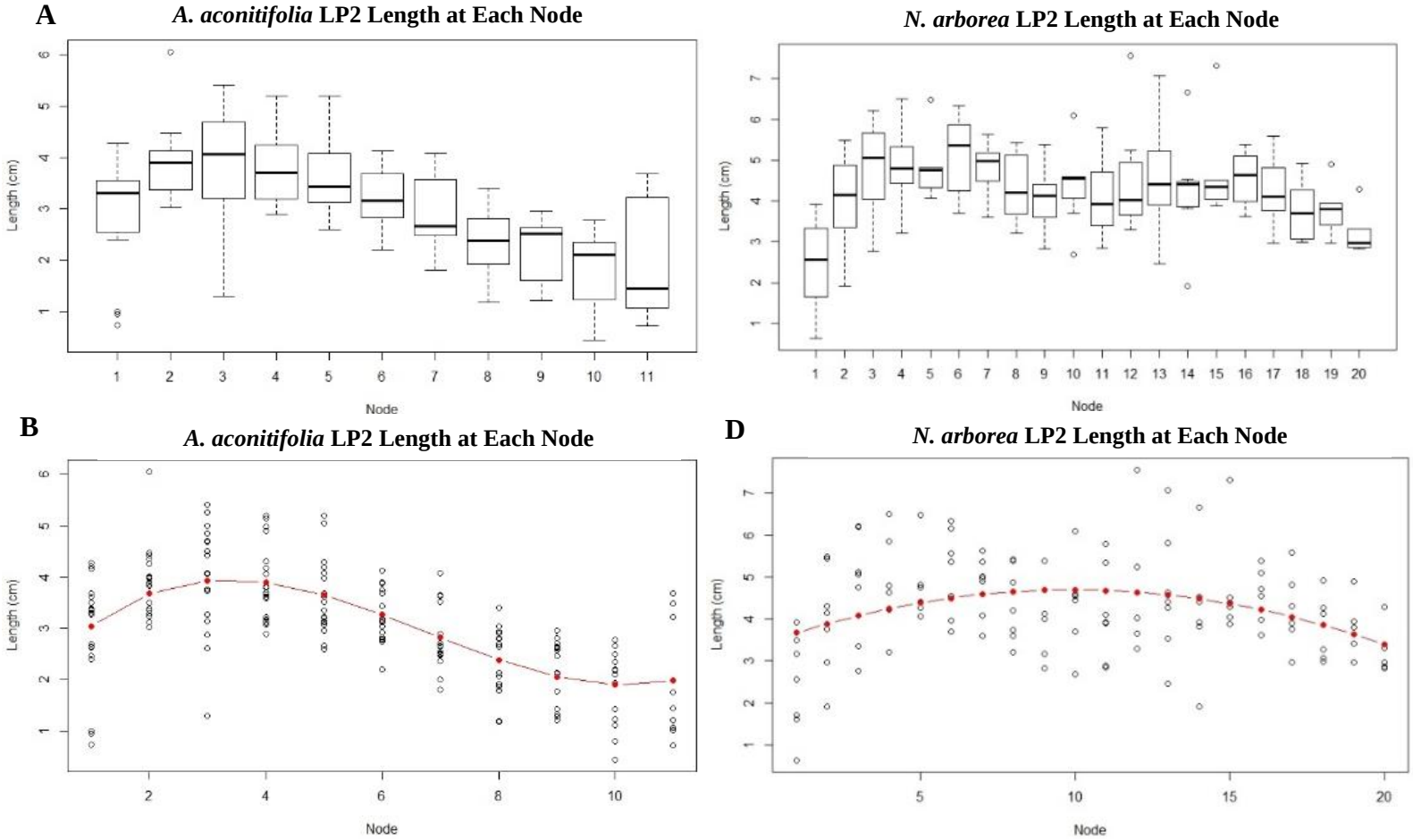

Figure 12: LP2 length at each node. (A) A boxplot showing the LP2 length in centimeters at each node along *A. aconitifolia* vines. (B) A scatterplot showing the LP2 length in centimeters at each node along *A. aconitifolia* vines with a regression line portraying the trend of the data shown in red ($p<0.0001$). (C) A boxplot showing the LP2 length in centimeters at each node along *N. arborea* vines. (D) A scatterplot showing the LP2 length in centimeters at each node along *N. arborea* vines with a regression line portraying the trend of the data shown in red ($p=0.0001$).

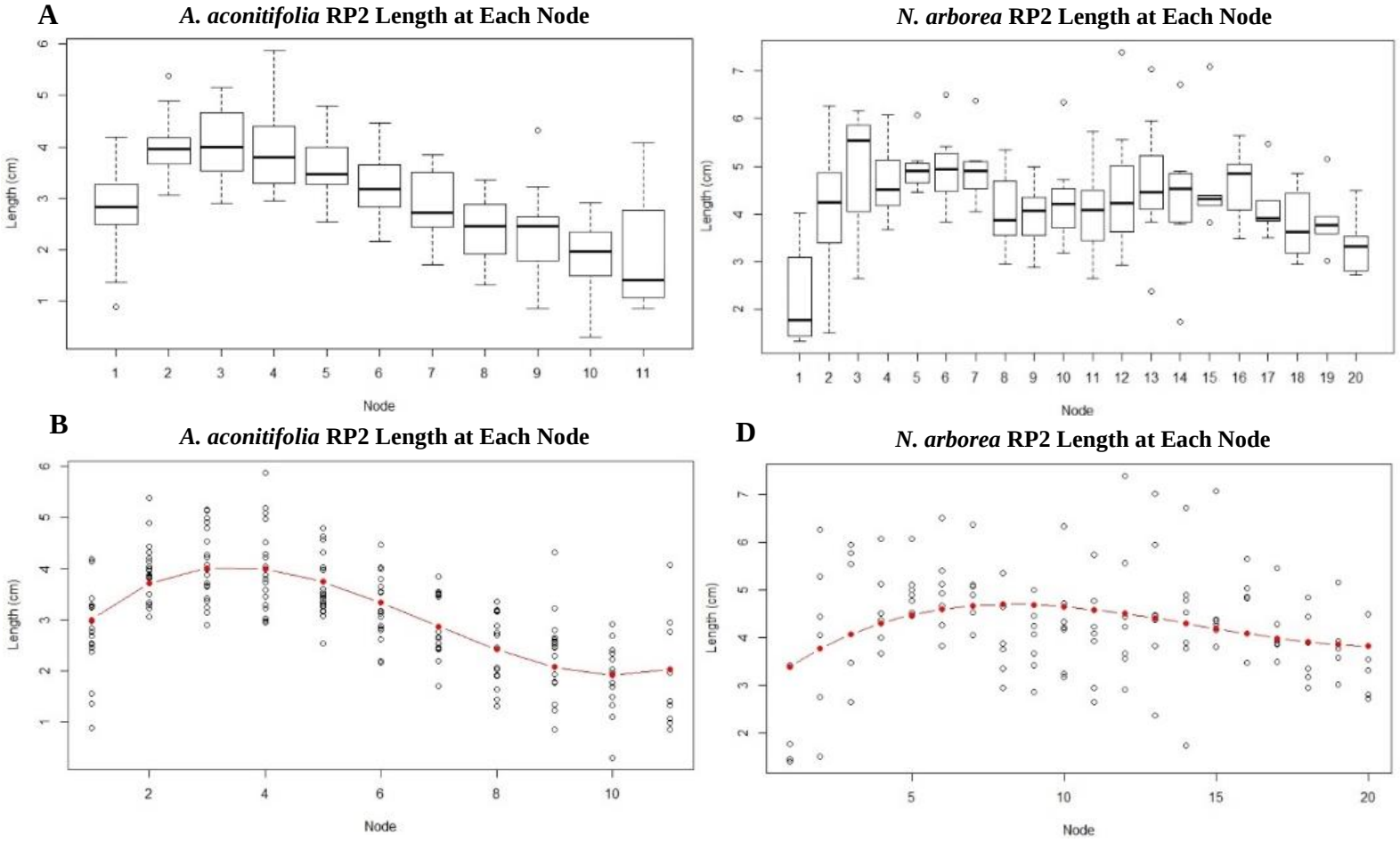

Figure 13: RP2 length at each node. (A) A boxplot showing the RP2 length in centimeters at each node along *A. aconitifolia* vines. (B) A scatterplot showing the RP2 length in centimeters at each node along *A. aconitifolia* vines with a regression line portraying the trend of the data shown in red ($p<0.0001$). (C) A boxplot showing the RP2 length in centimeters at each node along *N. arborea* vines. (D) A scatterplot showing the RP2 length in centimeters at each node along *N. arborea* vines with a regression line portraying the trend of the data shown in red ($p=0.0002$).

The trends of the RP2 length of *A. aconitifolia* leaves at each node were graphed and analyzed (Figure 13). For *A. aconitifolia,* both the boxplot and the regression line on the scatterplot show that there is a steady increase in average length which peaks at 4.06 cm at node three, after which there is a gradual decrease (Figure 13B-C). For *N. arborea,* both the boxplot and the regression line on the scatterplot show that there is a steady increase in average length with a peak at 4.94 cm around node seven (Figure 13E-F). More distally, length gradually decreases as the node number increases (Figure 13E-F).

The graphs showing the trend of the total leaf length of *N. arborea* leaves at each node were graphed and analyzed (Figure 14). Both the boxplot and the regression line on the scatterplot show that there is a steady increase in average total length and peaks at 11.61 cm on node seven (Figure 14B-C). Afterward, there is a gradual decrease in total length as the node number increases with a slight increase in perimeter again near the last node (Figure 14B-C).

LP3 and RP3 were only measured on *N. arborea* because *A. aconitifolia* stopped increasing in complexity after growing the LP2 and RP2 components of the leaf. Both graphs show the steady increase and peak, followed by the steady decrease in length (Figure 15). For both LP3 and RP3, length measurement values peaked around nodes six and seven and were 7.30 cm and 7.36 cm respectively (Figure 15).

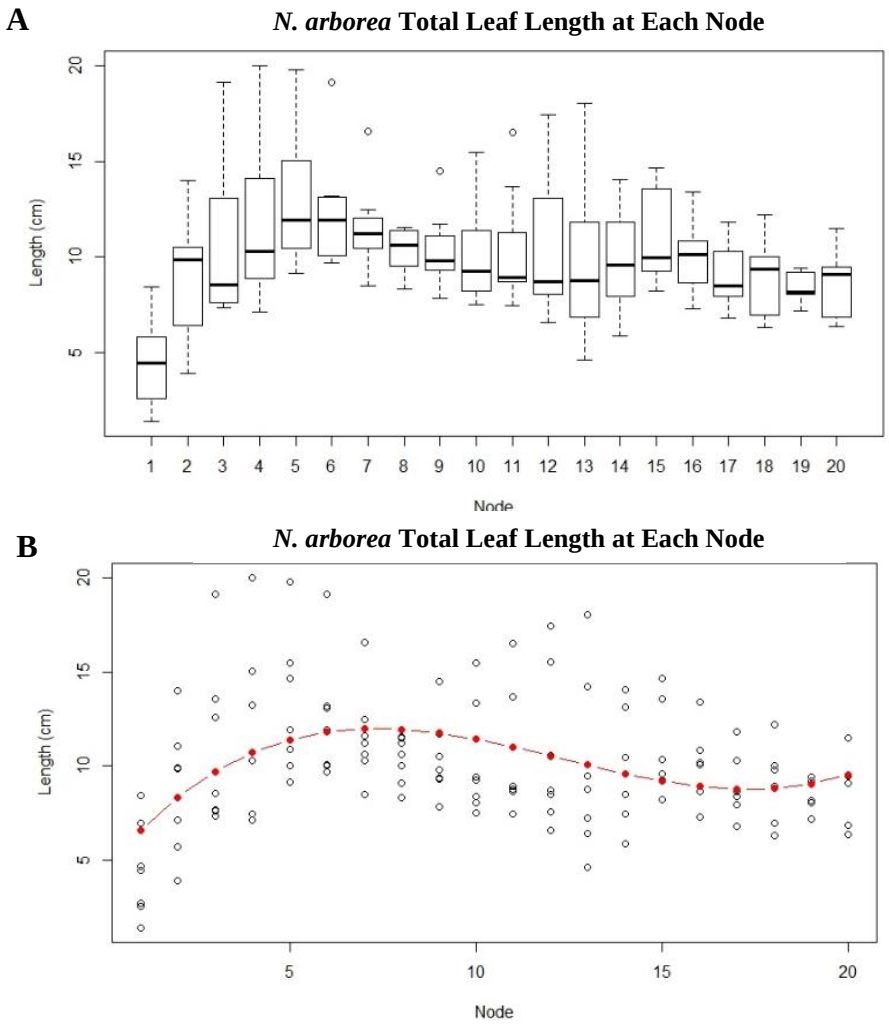

Figure 14: *N. arborea* leaf total leaf length at each node. (A) A boxplot showing the total leaf length in centimeters at each node along *N. arborea* vines. (B) A scatterplot showing the total leaf length in centimeters at each node along *N. arborea* vines with a regression line portraying the trend of the data shown in red ($p<0.0001$).

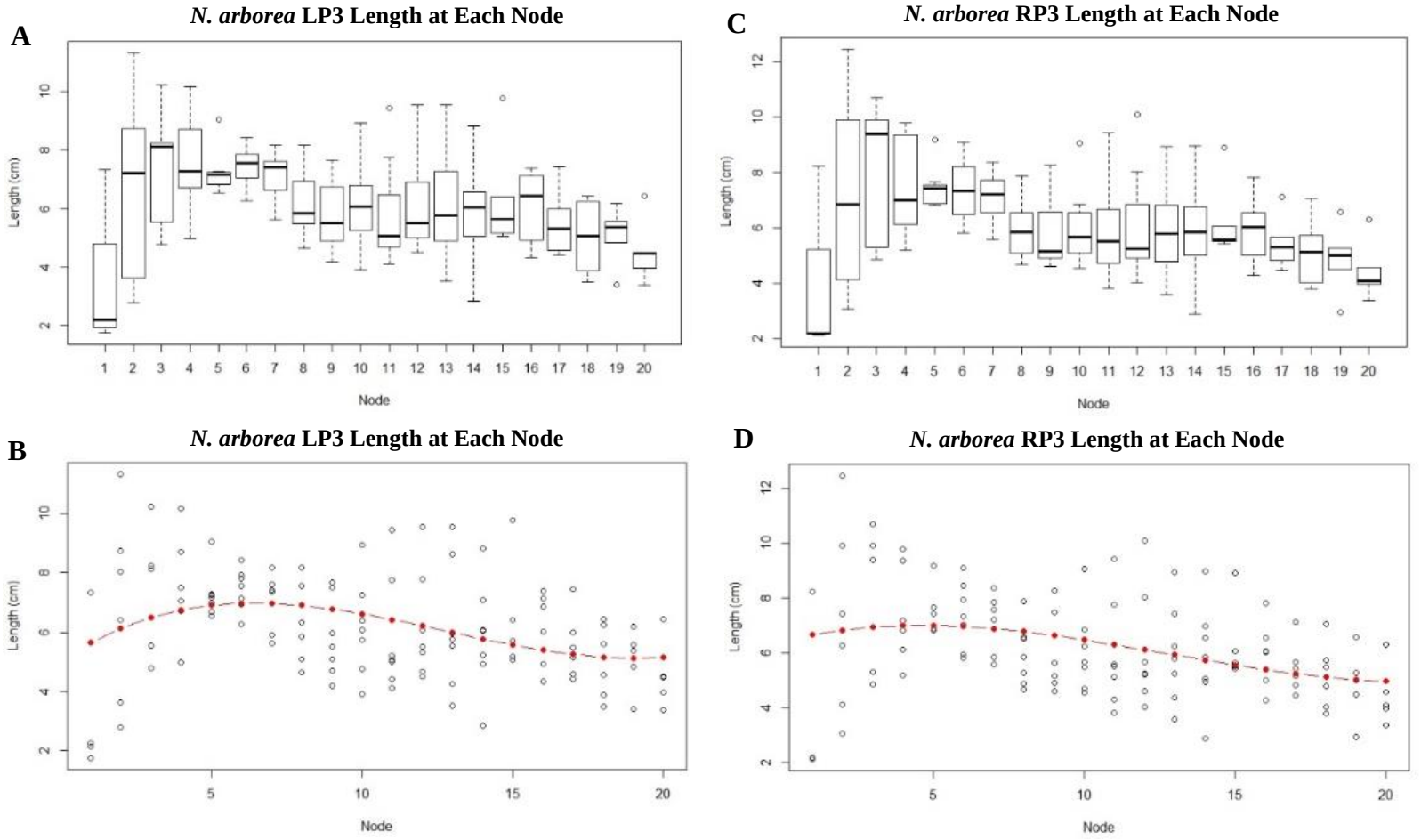

Figure 15: *N. arborea* LP3 and RP3 length at each node. (A) A boxplot showing the LP3 length in centimeters at each node along *N. arborea* vines. (B) A scatterplot showing the LP3 length in centimeters at each node along *N. arborea* vines with a regression line portraying the trend of the data shown in red ($p<0.0001$). (C) A boxplot showing the RP3 length in centimeters at each node along *N. arborea* vines. (D) A scatterplot showing the RP3 length in centimeters at each node along *N. arborea* vines with a regression line portraying the trend of the data shown in red ($p<0.0001$).

LP4 and RP4 were also only measured for *N. arborea* because they are not present in *A. aconitifolia.* The graphs showing the trend of the LP4 and RP4 lengths of *N. arborea* leaves at each node were analyzed and showed a different trend from previous variables (Figure 16). For the LP4 measurement, both the boxplot and the regression line on the scatterplot show a gradual decrease in length as the node number increases (Figure 16A-B). For the RP4 measurement, both the boxplot and the regression line on the scatterplot show that there is a gradual decrease in length as the node number increases (Figure 16C-D).

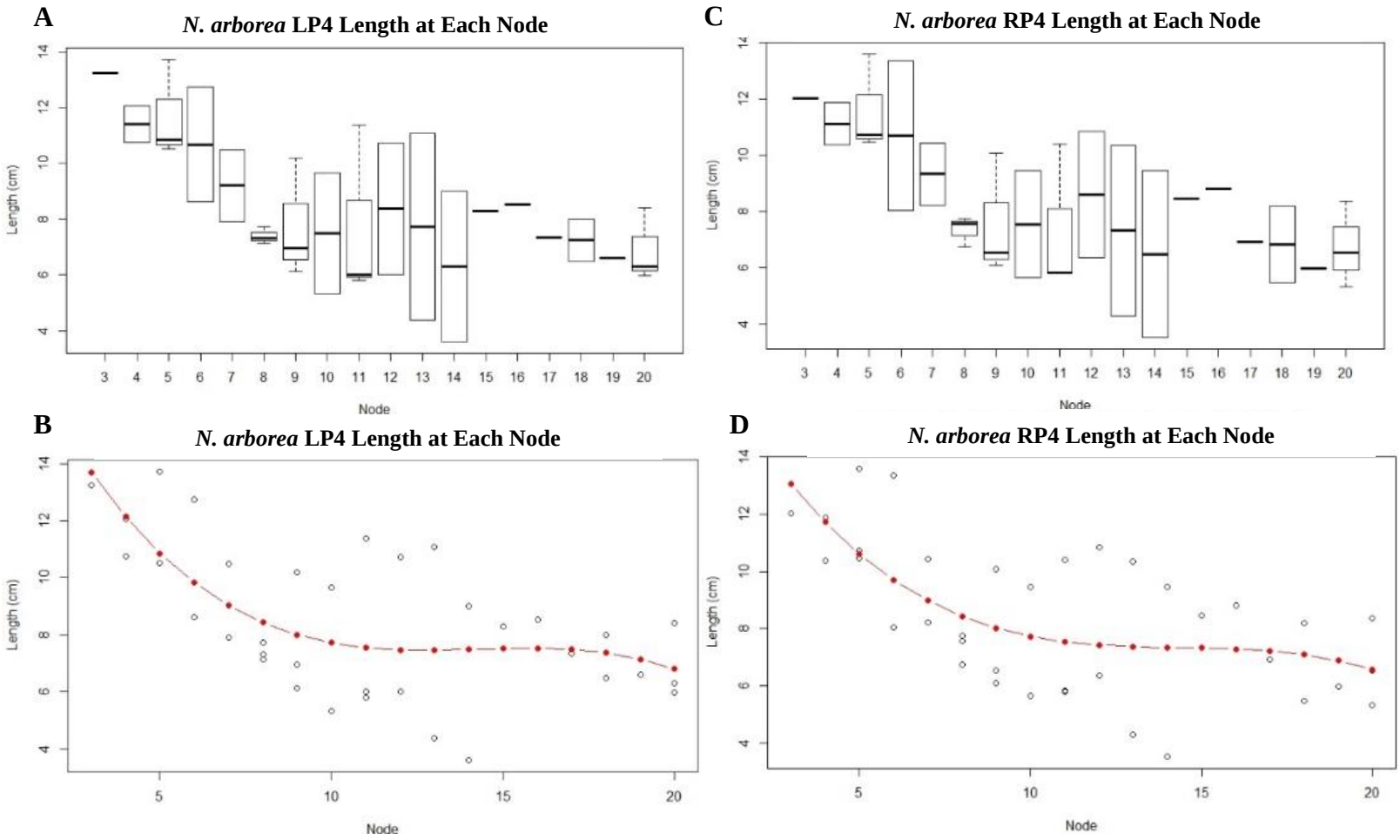

Figure 16: *N. arborea* LP4 and RP4 length at each node. (A) A boxplot showing the LP4 length in centimeters at each node along *N. arborea* vines. (B) A scatterplot showing the LP4 length in centimeters at each node along *N. arborea* vines with a regression line portraying the trend of the data in red ($p<0.0001$). (C) A boxplot showing RP4 length in centimeters at each node along *N. arborea* vines. (D) A scatterplot showing the RP4 length in centimeters at each node along *N. arborea* vines with a regression line portraying the trend of the data in red ($p<0.0001$).

Stem Structures

In addition to leaf shape trends along a vine, patterns of tendrils and lateral shoot initiation along the stems of each species were also assessed. A table showing tendril presence at each node and pattern at each plant was created (Appendix E). Both species show an alternate, distichous phyllotaxy (Figure 17A-B). The tendrils of both species were forked and occurred at the node on the opposite side of the stem from the leaf. Lateral shoots of both species were initiated out of the leaf axil (Figure 17C).

The *A. aconitifolia* vines grew to about eleven nodes before senescence. For 63.16% of plants, tendril presence began around node three. All remaining plants had tendrils begin forming at node four. After node three, tendrils were present at every single node, except for the last two or three nodes which contain inflorescences, which are modified tendrils on these species. Tendrils are forked and become woody after three or four weeks of growth. At every node that a tendril or inflorescence is present, an axillary bud is also present (Figure 17C). Presence of inflorescences was seemingly variable, with no visible pattern.

The *N. arborea* vines grew to about twenty nodes before senescence. For 71.43% of plants, tendril initiation began at nodes seven and eight. After node eight, tendrils were present on two successive nodes, skipped one node, then two successive nodes, and so on. Inflorescences in the form of modified tendrils mirrored that pattern on the final five or six nodes (Figure 17C).

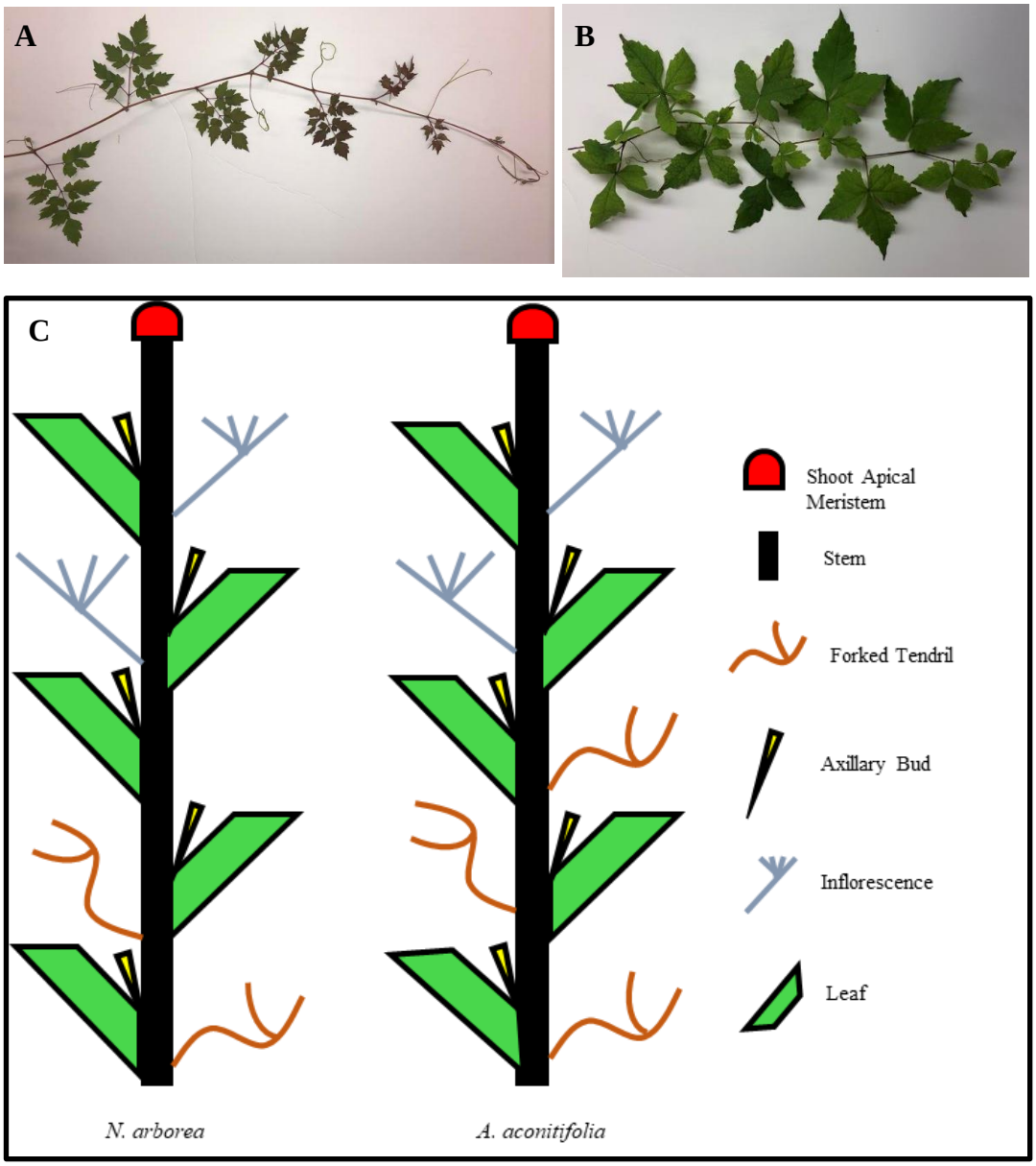

Figure 17: Vine structures and their arrangement along the vine. A) *N. arborea* vine showing shoot structure patterns. (B) *A. aconitifolia* vine showing shoot structure patterns. (C) Shoot patterns for both *N. arborea* and *A. aconitifoli*a. Figure legend is presented to the right.

CHAPTER 4

DISCUSSION

There is much that remains unknown about the Vitaceae. Its members' contribution to the wine industry retains much of the current focus of research. However, the *Vitis* species that contribute to the commercial grape industry make up only a small portion of the family. Thus, studying additional members of the grape family can help to elucidate the phylogenetic history and relationship with other plant families. Knowledge of the Vitaceae will also contribute to what scientists know about growth patterns and structure development in climbing lianas (Sousa-Baena et al. 2014; Sousa-Baena et al. 2018). Similarities observed in leaf development between species may also give information about the phylogenetic relationships between members of the Vitaceae (Gerrath and Lacroix 1997; Costa et al. 2012; Geeta et al. 2012; Cho et al. 2016; Spriggs et al. 2018; Tsukaya et al. 2018). If specific developmental stages in the Vitaceae are composed of leaves or leaf primordia of the same level of complexity, relationships between members may be hypothesized. For example, if a bipinnately compound species (such as *Nekemias arborea)* shares only early structural similarities in the leaf primordia with another species in the same family (such as *Ampelopsis aconitifolia*) that has simple or palmately compound leaves, it could be hypothesized that the bipinnately compound species shares more similarities with the bipinnate outgroup than the palmately compound species does. This is especially possible in a family with so many leaf forms, which could imply a high rate of evolutionary change between the varying morphologies.

Leaf similarities and differences could help establish relationships between genera in a family with such plasticity in leaf form.

The purpose of this study was to investigate leaf development and stem structures and their relationship to tendril formation in *Ampelopsis aconitifolia* and *Nekemias arborea.* These two species were selected based on their contrasting leaf morphology, one being dissected and the other highly compound. Scanning electron microscopy was used to observe early leaf development while ampelography and morphometrics were used to examine leaf growth along the vine. Developmental patterns of the leaves were analyzed with respect to stem structures and tendril formation to determine correlations between these developmental traits.

Shoot apical meristems (SAMs) of both species were collected and analyzed to establish and compare the stages of leaf development. It was found that leaf development was similar between the species from P1 to P2 stages (Appendix B). Leaves from both species initiated as small protrusions from the meristem and next developed a pair of lateral primary leaflets below the terminal leaflet (Appendix B). It is at the P3 and P4 stages that the two species diverged in their leaf development. Where *A. aconitifolia* leaves stopped increasing in complexity after the development of a second pair of primary lateral leaflets, *N. arborea* continued to develop two more pairs of primary lateral leaflets as well as secondary leaflets (Figures 5 and 6). Observations by Jones et al. (2013), showed that the simple-leafed species *A. cordata* and the compound-leafed *N. arborea* morphology were only similar at early leaf developmental stages (up to P2). This similarity may be explained by a discovery by Gerrath and Lacroix (1997), that the

terminal leaflets in pinnately compound leaves are homologous to the simple leaf form. Because the most mature, compound leaf can be related back to its simple juvenile form, the leaf primordia in the Vitaceae at initiation can be very similar but diverge later on. Beyond the P2 stage, leaf shape clearly diverged between *A. cordata* and *N. arborea* (Jones et al. 2013).

The fact that we observed divergence of leaf shape in both species at later stages (P3 and P4) may be due to the prolonged cell division activity along the leaf margin resulting in dissected leaves (Figures 5 and 6). After a leaf primordium is initiated, a region of cells along the edge of the new organ, called the blastozone, retains its meristematic activity (Hagemann and Gleissberg 1996). As the primordium continues to develop, a process called blastozone fractionation occurs. Blastozone fractionation involves localized enhancement and suppression of growth on specific areas of the leaf margin (Gunawardena and Dengler 2006). The rates and locations of these fractionation events can cause a wide variety of leaf complexities (Dengler and Tsukaya 2001). If the activity of the blastozone is prolonged, as can be caused by initiation of structures such as tendrils, there is more time for fractionation, which may result in a more dissected, more compound leaf. If the marginal blastozone is not very active, the leaf will develop to be more simple in shape (Hagemann and Gleissberg 1996).

Studies have shown that angiosperms have a strong tendency to retain or re-evolve simple leaf forms, with lobed leaves acting as the intermediate form between simple and complex when rate of evolutionary change is high (Sherry and Lord 1996). In the case of the Vitaceae, it has been hypothesized that the ancestral leaf form was

compound (Bharathan 2002). Since there are both simple- and compound-leafed members of the family, this suggests that some may have reverted back to simple leaf-forms while others have not. In this study, both a highly compound-leafed species (*N. arborea*) versus a less complex, simple to deeply dissected species (*A. aconitifolia*), were studied. When compared to the outgroup, *Leeaceae, N. arborea* harbors many similarities, with an abundance of lateral primary leaflets as well as secondary leaflets (Figure 3) (Gerrath and Lacroix 1997). Leeaceae is a monogeneric family in Australia, Asia, and Africa that is composed of trees or shrubs that can be simple, trifoliate, or bipinnately compound and is considered very closely related to Vitaceae, in the past being referred to as a subfamily or tribe (Ridsdale 1974; Wen 2007). It is possible that by comparing and contrasting Leeaceae to the Vitaceae, scientists can gain a better understanding of the common ancestry of both, and thus how the Vitaceae may have evolved to be where they are now morphologically. The rest of the *Ampelopsis* clade, besides *N. arborea*, has made a transition from the compound ancestral leaf form to simpler structures. *A. aconitifolia* shows little similarity to Leeaceae in the adult form, despite sharing some similarity with *N. arborea* in early primordial stages (Figure 3). The deeply dissected/palmately lobed leaf structures of *A. aconitifolia* serves as the intermediate between the complex to simple transition it may be making. This is an important observation because it reveals *A. aconitifolia* having the derived leaf form compared to *N. arborea's* conserved form. This information helps to contribute to the discovery of the evolutionary history of the Vitaceae. Discovering conserved versus derived traits gets researchers closer to a depiction of what the common ancestors of the

clades and family might have looked like. Consequently, knowing which plants are more closely related to one another will help to determine which plants can be used to solve any diseases or similar problems that may arise in the other closely related members of the family.

Ampelography deals with creating horticultural descriptions of grape plants, specifically leaves of Vitis (Bioletti 1938; Dexheimer 2011; Schneider et al., 1996; Tassie 2010). This method analyzes leaf shape and size by measuring different characteristics, such as leaf length, vein length, serrations, or angles between veins (Tassie 2010; Alba et al. 2011). These measurements allow leaves to be compared to others along the same vine, those of other related plants, and to those of other species (Chitwood et al. 2016; Klein et al. 2017; Migicovsky et al. 2018). Based on the information that could be extracted from analyzing characteristics of a leaf, ampelography was used in this study to provide information about leaf shape relationships between the two species (Alba et al. 2011). Measurements that were taken on all leaves were area, perimeter, midvein length, and length of all primary leaflets (Figure 2). The angle between leaflets was also measured but found to be subjective depending on how the leaves were laid down for photography (Appendix C). Regardless, of all other measurements taken, there was a distinct trend in the leaf data for both species (Figure 7-16). Other than the position of the peak, the trend of a gradual increase followed by a gradual decrease in measurement size was consistent across species. All measurements for both species showed a gradual increase in value to a peak at a specific node and then a gradual decline in value. This includes area, perimeter, midvein length, and all primary leaflet vein lengths (Figure 2).

For *A. aconitifolia,* that peak occurred at nodes three and four (Figure 6-12). For *N. arborea,* that peak occurred at nodes seven and eight (Figure 6-15). A similar pattern exists regarding the serrations on the margins of the leaves of both species, with serrations increasing in number and becoming more saw-toothed at an early node and later reverting back to their original state near the end of the vine (Figure 4). This pattern of serration presence along the vine corresponds with the presence of tendrils. Because tendrils signify that the vine has reached maturity, it could be said that serration number is increased in the adult leaf and decreased in the juvenile form (Sousa-Baena et al. 2018).

There are many factors which can affect leaf proportions such as genes, hormones, environmental factors, or developmental stages that can influence cell division, cell growth, and organ initiation (Fishel 2006; Spriggs et al. 2018; Tsukaya 2004). The changes observed in my study may be explained by the presence of hormones that act as either growth inhibitors or growth stimulants. While growth inhibitors and stimulants were not tested in this study, it can be hypothesized that they may have some effect on leaf morphology. For example, presence of growth regulators were found to have an effect on leaf size (Coombe 1967; Gaspar et al. 1996; Achard et al. 2006). Growth inhibitors can slow or alter the normal growth process, resulting in changes such as thickened stems, decreased fruit yield, smaller leaves, or promotion of flower initiation (Bennett and Bonner 1953; Cathey 1964; Grossmann 1990; Rademacher 2000). Ninnemann et al. (1964) discovered that adding 10 mg/L of the plant growth retardant, CCC [(2-chloroethyl) trimethylammonium chloride], to the growth medium of *Fusarium*

moniliforme fully suppressed production of gibberellic acid (GA), a plant growth stimulant (Ninnemann et al. 1964). This results in the reduction in plant height and leaf number (Zeevart et al. 1964). Experiments such as those done by Ninnemann et al. (1964) show how important plant genes and hormones are to the natural development of plants and that altering their levels can change the morphology of the organism.

Patterns of leaf development along the vine may be explained by changes in growth regulator levels at the time of leaf initiation. Gibberellic acid is a phytohormone found in plants and fungi and is produced naturally by plants but can also be produced synthetically, often used in the commercial industry to produce larger bundles of bigger grapes (Pharis et al. 1985; Abu-Zhara 2010; Casanova et al. 2009; Dokoozlian and Peacock 2001; Pérez and Gómez 2000). Tests on a variety of plants, including legumes and tomatoes, have shown that treating the meristem with GA increases the length and width of the leaves (Gray 1957; Marth et al. 1956). The treatment to achieve this leaf growth was accomplished by spraying 10—100 p.p.m. GA on the shoot apical meristem during leaf primordium development (Gray 1957).

Giberellic acid is important in seed germination, growth of stems and leaves, and floral transition (Davière and Achard 2013). In order to promote leaf growth, GA interacts with DELLA proteins (Gupta and Chakrabarty 2013). DELLA proteins are transcriptional regulators responsible for inhibiting cell proliferation and growth of organs, including leaves (Alvey et al. 2005). GA promotes DELLA destruction, allowing for cell division and growth, which results in larger leaf measurements (Davière and Achard 2013). Thus, the influx of GA into the SAM for initiation of tendrils could cause

a long-lasting, but not permanent change in leaf morphology along the vine (Maksymowych and Maksymowych 1973). Because gibberellic acid is also a growth stimulant, it may be responsible for the increase and peak in leaf size measurements affecting the heteroblastic series in this study (Brian 1959). The gradual decline in leaf size at all variables may be explained by a possible decrease in GA and by the age of the vine. Toward the apical end of the vine, reproductive activation and beginning of senescence occur. As the plant readies for inflorescence production, nutrients are cycled to other parts of the plant besides the leaf. In order for optimal reproductive success, the plant must allocate more resources to floral development than to leaf growth (Gan and Amasino 1997).

It is known that serration number in plant margins is affected by the expression of the microRNA, *miR319,* and its target genes, the *TEOSINTE BRANCHED1/CYCLOIDEA* and *PROLIFERATING CELL NUCLEAR ANTIGEN BINDING FACTOR* (*TCP)* (Czesnick and Lenhard 2015). These target genes are part of a transcription factor family collectively referred to as the *TCP* family (Ballester et al. 2015). In tomato plants, it has been shown that *miR319* is a negative regulator of *LANCEOLATE (LA)*, a member of *TCP*, which restricts morphogenic activity in the marginal blastozone (MB), or leaf margin (Ben-Gera and Ori 2012; Nardmann and Werr 2007). An increase in the hormone cytokinin restricts the activity of *miR319* and the *TCP* family which, as a result, restricts the activity of *LA* (Bar and Ori 2014). The end product of this cascade is the lack of restriction of morphogenic activity in the leaf margin, leading to an increase in leaf serrations (Efroni et al. 2008). Additionally, cytokinin is also required for the initiation of

tendrils and inflorescences (Srinivasan and Mullins 1980). In this study, it was found that both plant species exhibited an increase in the number of serrations on the leaf margins as node number increased. For *A. aconitifolia*, this increase occurred at node three (Figure 3A). For *N. arborea*, this increase occurred at node eight (Figure 3B). Therefore, it is possible that cytokinin, along with the aforementioned genes, may be responsible for the increased serration number at the same node where tendril initiation occurs.

Studies on tomato plants have also shown that cytokinin levels can play a role in the development of more complex leaves (Shani et al. 2010). *LANCEOLATE (LA)* of the TCP family negatively controls the shoot apical meristem by encouraging differentiation (Koyama et al. 2010; Ikeda and Ohme-Takagi 2014). Thus, the presence of cytokinin in developing leaf primordia, as well as its downregulation in certain areas of the leaf primordia, results in a more complex leaf shape (Efroni et al. 2008; Koyama et al. 2017; Ori et al. 2007; Palatnik et al. 2003). The presence of cytokinin may explain the simultaneous increase in serration number and leaf complexity in the *N. arborea* and *A. aconitifolia* plants evaluated in this study (Floyd and Bowman 2010; Hagemann and Gleissberg 1996).

While cytokinin, along with *KNOX1 (KNOTTED-LIKE HOMEOBOX 1 GENE)*, may be responsible for an increase in leaf complexity, the plant hormone auxin is required to determine the sites where leaves and leaflets are initiated (Hamant et al. 2008; Barkoulas et al. 2008; Blein et al. 2010; Canales and Martínez 2010). Auxins are required for plant growth, leaf development, vein structure, and are found in shoot and root tips (Shwartz et al. 2016; Scarpella et al. 2017). They promote cell division, shoot elongation,

orientation of structures, and regulate other plant hormones (Jenik and Barton 2005; Joo et al. 2001; Ludwig-Müller 2011; Zhao 2010). Auxins promote the actions of GA and interact with cytokinin in many of its functions including meristem formation and organ formation (Su et al. 2011). Auxin and GA together interact with the *Unifoliata* (*UNI*) gene in pea (DeMason and Chetty 2011). The *UNI* gene regulates leaf dissection and is upregulated by GA and auxin (DeMason and Chetty 2011). This prolongs the period of time in which leaflets are initiated, allowing for the production of more complex leaf forms. This may also account for the increase in complexity in leaf form on *N. arborea* and *A. aconitifolia* vines after an influx of auxin and GA initiate leaf and tendril formation (Cheng and Zhao 2007).

While cytokinin and GA are present in more distal buds, the hormone abscisic acid (ABA) is also found in those regions (Finkelstein 2013). Abscisic acid is a phytohormone required for the initiation of the flowering process and abscission of the leaves (Leung and Giraudat 1998). Abscisic acid is produced in the last few buds on the vine to prepare the plant for flowering and dormancy during the winter by acting as a GA antagonist, therefore interfering with cell duplication and elongation, causing the stunting of leaf growth (Nambara and Marion-Poll 2005). Although ABA is present in the early vine and helps with initial leaf growth, the environmental changes that accompany approaching winter as well as the stresses of an aging vine alter the function of the phytohormone from stimulatory to inhibitory (Skriver and Mundy 1990). It is possible then that ABA may be responsible for the gradual decline in leaf size near the end of the vine.

The reversion back to rounded leaves with fewer serrations at the last three nodes of *N. arborea* can also be explained by changes in ABA levels. As the vine becomes longer and nears the end of growth, cytokinin and GA, which play a role in promoting cell proliferation and may be responsible for increased serrations, are counteracted by ABA (Nambara and Marion-Poll 2005). This pathway results in a slow reversion back to rounded leaves with fewer serrations (Efroni et al. 2013). Serrations in *A. aconitifolia* do not return to their earlier form, possibly because the vines contain over 50% fewer nodes and have terminated growth or begun to senesce before any reversion could take place. This suggests that vine elongation and leaf expansion has terminated before the plant is close to dormancy, avoiding any rise in ABA levels. The serrations along the leaf margins have fully formed while GA levels were still uninhibited.

The idea that phytohormones may be closely linked to the leaf morphology of these plants could be helpful in forming relationships between them. *N. arborea* and *A. aconitifolia* both have changing patterns of leaf morphology that is correlated with tendril presence and absence. Although their tendril patterns have diverged from one another, they do retain the same patterns in complexity and size changes along the vine. Because most members of Vitaceae have tendrils, the pattern of leaf morphology changing with tendril presence could be a theme for the family, either retained from the common ancestor with Leeaceae or developed afterward. The leaf-opposed location of the tendrils is distinctive to Vitaceae, but the branching pattern has evolved multiple times and is unreliable as a phylogenetic indicator (Gerrath et al. 2001; Wen et al. 2007; Lu et al. 2013). This growth pattern has not been well researched in Vitaceae but future research

on phytohormones during tendril development may be helpful. Additionally, even though Leeaceae members do not have tendrils, phytohormones may be acting to control compound leaf development.

The United States exported $903.4 million worth of fresh grapes and $1.53 billion worth of wine in 2017. The grape industry provides food products, employment opportunities, tourism opportunities, tax revenue, export profits, and more (Initiative 2007). Research on the factors that affect leaf shape and complexity could be used agriculturally on the commercially-used members of the family to maintain plant health. With leaves being the energy producers for the organism and the location of sugar production, they are important to the growth and quality of the fruits cultivated. For example, a recent study on tomato plants showed that the shape of a leaf can strongly impact the flavor and yield of the fruit. By doing a BRIX and yield analysis as well as taking various morphological measurements, researchers were able to determine that plants with rounder, less lobed leaves produced more grapes with higher sugar content (Rowland et al. 2019). This shows that research into leaf shape and shape change throughout the family may reveal information that helps improve fruit yield and quality. In addition, knowing the factors affecting the leaf form and leaf health can allow researchers to solve problems like the phylloxera outbreak before they cause major harm to the crop (Sinnott 1923). Knowing how to optimize overall plant health and fruit yield by understanding factors contributing to leaf shape and development can help boost the success of the grape industry and, consequently, the economy.

The phylogenetic history of Vitaceae and how it correlates with Leeaceae is helpful in continuing scientists' ongoing work into documenting the history of the angiosperms. The plant world is what balances out the oxygen reliant organisms. Without the establishment and success of the botanical world, the atmosphere would no longer be a suitable habitat for life on Earth (Veron 2008). The diversity of this vital plant world is difficult to comprehend and difficult to unravel. The only method we have to uncover the history of this diversity is to look at the plants that exist now and work backwards to analyze the past. By looking at current members of the grape family, the characteristics of their ancestors will become evident. To do this, leaf development, size, and complexity can be analyzed and compared with members within and outside the Vitaceae, to establish which species are more closely related and determine what morphological characteristics are derived or conserved. Because of their commercial importance, the agriculturally-grown grapes have received the vast majority of the attention from researchers, however information about related species can be used to help improve and problem solve our uses of grapes for food, flavoring, and wine by combatting disease or increasing fruit production. Work on the more obscure family members like *N. arborea* and *A. aconitifolia* should not be ignored, as it bares more importance than often predicted.

Future Research

There are many factors regarding the relationship between *N. arborea, A. aconitifolia,* and other members of the grape family that can still be investigated to clarify existing questions. Because the research on this family is relatively sparse compared to other families, more research can be done. Both molecular and morphological traits of the genera within Vitaceae can be conducted to reveal the evolution of leaf complexity and patterns in leaf form.

One avenue that can be further explored is phytohormone levels within the shoot apical meristem and leaves during leaf primordium initiation and formation. Knowing the presence or absence and volume of growth inhibitors or stimulants may help to explain the gradual increase, peak, and gradual decrease of leaf size along the vines of *N. arborea* and *A. aconitifolia.* Testing these hormones may help to elucidate the patterns of leaf development assessed in this study.

Another area that can be investigated is advancing morphometric capabilities in regard to very complex, compound leaves like those of *N. arborea.* Two difficulties were encountered with the bipinnately compound leaves of this species: The first was that morphometric programs like SHAPE failed to recognize the rachis of the leaf as well as leaf dissections extending very close to the rachis. To overcome this issue, bitmap plates were created of leaves from each species but were not analyzed using the morphometric program (Appendix F).

The second issue that arose was regarding the lack of pattern in the emergence of secondary leaflets. This is similar to the variability in leaf form that makes tomato plants

difficult to study from a morphometrics and landmarking standpoint. Because of the variability in location and number of secondary leaflets, landmark analysis of anything more than just the primary leaflets was not achieved.

There is much more research to be done beyond *N. arborea* and *A. aconitifolia.* There are other members of Vitaceae that can be compared and contrasted with each other to reveal morphological patterns within the family. Species with simple leaves, such as *Ampelopsis cordata*, and other species with complex leaves, such as the pinnately-compound *A. megallophylla*, can be compared with one another as well as with the species analyzed in my research to uncover the history of leaf form in the family. Vine structures such as tendrils can also be compared between more members of Vitaceae to determine what effects they may have on the heteroblasty of other species. These tendrilled species can later be compared to the outgroup, Leeaceae, which lacks tendrils. Involving more species in the research process will provide a more complete picture of the history of the Vitaceae.

REFERENCES

Abu-Zahra TR. 2010. Berry size of Thompson seedless as influenced by the application of gibberellic acid and cane girdling. *Pak J Bot*, *42*(3), 1755-1760.

Achard P, Cheng H, De Grauwe L, Decat J, Schoutteten H, Moritz T, Harberd NP. 2006. Integration of plant responses to environmentally activated phytohormonal signals. *Science*, *311*(5757), 91-94.

Adams DC, Rohlf FJ, Slice DE. 2004. Geometric morphometrics: ten years of progress following the 'revolution'. *Italian Journal of Zoology*, *71*(1), 5-16.

Alvey L, Harberd NP. 2005. DELLA proteins: integrators of multiple plant growth regulatory inputs. *Physiologia Plantarum, 123*(2), 153-160.

Ballester P, Navarrete-Gómez M, Carbonero P, Oñate-Sánchez L, Ferrándiz C. 2015. Leaf expansion in *Arabidopsis* is controlled by a TCP-NGA regulatory module likely conserved in distantly related species. *Physiologia plantarum*, *155*(1), 21-32.

Banerjee A, Duflo E, Postel-Vinay G, Watts T. 2010. Long-run health impacts of income shocks: Wine and phylloxera in nineteenth-century France. *The Review of Economics and Statistics, 92*(4), 714-728.

Bar M, Ori N. 2014. Leaf development and morphogenesis. *Development*, *141*(22), 4219-4230.

Barkoulas M, Hay A, Kougioumoutzi E, Tsiantis M. 2008. A developmental framework for dissected leaf formation in the Arabidopsis relative Cardamine hirsuta. *Nature Genetics*, *40*(9), 1136.

Ben-Gera H, Ori N. 2012. Auxin and LANCEOLATE affect leaf shape in tomato via different developmental processes. *Plant Signaling & Behavior*, *7*(10), 1255-1257.

Bennett EL, Bonner J. 1953. Isolation of plant growth inhibitors from Thamnosma montana. *American Journal of Botany, 40*(1), 29-33.

Bharathan G. 2002. Homologies in Leaf Form Inferred from KNOXI Gene Expression During Development. *Science*, *295*(5574), 1858-1860. doi:10.1126/science.1070343

Bioletti F. 1938. Outline of ampelography for the *vinifera* grapes in California. *Hilgardia, 11*(6), 227-293.

Blein T, Hasson A, Laufs P. 2010. Leaf development: what it needs to be complex. *Current opinion in plant biology, 13*(1), 75-82.

Bongard-Pierce DK, Evans MMS, Poethig RS. 1996. Heteroblastic features of leaf anatomy in maize and their genetic regulation. *International Journal of Plant Sciences, 157*(4), 331-340.

Brian PW. 1959. Effects of gibberellins on plant growth and development. *Biological Reviews, 34*(1), 37-77.

Calonje M, Cubas P, Martínez-Zapater JM, Carmona MJ. 2004. Floral meristem identity genes are expressed during tendril development in grapevine. *Plant Physiology, 135*(3), 1491-1501.

Canales AR, Martínez JMM. 2010. Automatización y telecontrol de sistemas de riego. Marcombo.

Casanova L, Casanova R, Moret A, Agustí M. 2009. The application of gibberellic acid increases berry size of "Emperatriz" seedless grape. *Spanish Journal of Agricultural Research, 7*(4), 919-927.

Cathey HM. 1964. Physiology of growth retarding chemicals. *Annual Review of Plant Physiology, 15*(1), 271-302.

Champagne CE, Goliber TE, Wojciechowski MF, Mei RW, Townsley BT, Wang K, Sinha NR. 2007. Compound leaf development and evolution in the legumes. *The Plant Cell, 19*(11), 3369-3378.

Cheng Y, Zhao Y. 2007. A role for auxin in flower development. *Journal of Integrative Plant Biology, 49*(1), 99-104

Chitwood DH. 2015. Developmental Stability of Grape Leaf Morphometrics: Allometry, Heteroblasty, and Interannual Variability of *Vitis* spp. DDPSC REU Program

Chitwood DH, Headland LR, Filiault DL, Kumar R, Jiménez-Gómez JM, Schrager AV, Maloof JN. 2012. Native environment modulates leaf size and response to simulated foliar shade across wild tomato species. *PLoS One, 7*(1), e29570.

Chitwood DH, Klein LL, O'Hanlon R, Chacko S, Greg M, Kitchen C, Londo JP. 2016. Latent developmental and evolutionary shapes embedded within the grapevine leaf. *New Phytologist*, 210(1), 343-355.

Chitwood DH, Otoni WC. 2017. Morphometric analysis of *Passiflora* leaves: the relationship between landmarks of the vasculature and elliptical Fourier descriptors of the blade. *GigaScience, 6*(1), giw008.

Chitwood DH, Ranjan A, Martinez CC, Headland LR, Thiem T, Kumar R, Downs N. 2014. A modern ampelography: a genetic basis for leaf shape and venation patterning in grape. *Plant Physiology, 164*(1), 259-272.

Cho SH, Lee JH, Kang DH, Kim BY, Trias-Blasi A, Htwe KM, Kim YD. 2016. *Cissus erecta* (Vitaceae), a new non-viny herbaceous species from Mt. Popa, Myanmar. *Phytotaxa*, 260(3), 291-295.

Coombe BG. 1967. Effects of growth retardants on *Vitis vinifera*. *Vitis, 6*, 278-287.

Costa MMR, Yang S, Critchley J, Feng X, Wilson Y, Langlade N, Hudson A. 2012. The genetic basis for natural variation in heteroblasty in *Antirrhinum*. *New Phytologist, 196*(4), 1251-1259.

Czesnick H, Lenhard M. 2015. Size control in plants—lessons from leaves and flowers. *Cold Spring Harbor Perspectives in Biology, 7*(8), a019190.

Davière JM, Achard P. 2013. Gibberellin signaling in plants. *Development, 140*(6), 1147-1151.

Dengler NG, Tsukaya H. 2001. Leaf morphogenesis in dicotyledons: current issues. *International Journal of Plant Sciences, 162*(3), 459-464.

Dexheimer F. 2011. The Science of Ampelography. *Sommelier Journal, 6*(4), 87-91.

DeMason DA, Chetty VJ. 2011. Interactions between GA, auxin, and UNI expression controlling shoot ontogeny, leaf morphogenesis, and auxin response in *Pisum sativum* (Fabaceae): Or how the uni-tac mutant is rescued. *American Journal of Botany*, 98(5), 775-791.

Díaz-Riquelme J, Martínez-Zapater JM, Carmona MJ. 2014. Transcriptional analysis of tendril and inflorescence development in grapevine (*Vitis vinifera* L.). *PLoS One, 9*(3), e92339.

Dokoozlian NK, Peacock WL. 2001. Gibberellic acid applied at bloom reduces fruit set and improves size of 'Crimson Seedless' table grapes. *HortScience, 36*(4), 706-709.

Efroni I, Han SK, Kim HJ, Wu MF, Steiner E, Birnbaum KD, Wagner D. 2013. Regulation of leaf maturation by chromatin-mediated modulation of cytokinin responses. *Developmental cell, 24*(4), 438-445.

Finkelstein R. 2013. Abscisic acid synthesis and response. *The Arabidopsis book/American Society of Plant Biologists, 11*.

Fishel FM. 2006. Plant growth regulators. Document PI-139, Pesticide Information Office, Florida Cooperative Extension Service, Institute of Food and Agricultural Sciences, University of Florida.

Floyd SK, Bowman JL. 2006. Distinct developmental mechanisms reflect the independent origins of leaves in vascular plants. *Current Biology*, *16*(19), 1911-1917.

Floyd SK, Bowman JL. 2010. Gene expression patterns in seed plant shoot meristems and leaves: homoplasy or homology? *Journal of Plant Research, 123*(1), 43-55.

Forster M, Sober E. 2011. AIC scores as evidence—a Bayesian interpretation. na.

Galet P. (1952). Precis D'Ampelographie Pratique (Par).

Gan S, Amasino RM. 1997. Making sense of senescence (molecular genetic regulation and manipulation of leaf senescence). *Plant Physiology*, *113*(2), 313.

Geeta R, Dávalos LM, Levy A, Bohs L, Lavin M, Mummenhoff K, Wojciechowski MF. 2012. Keeping it simple: flowering plants tend to retain, and revert to, simple leaves. *New Phytologist, 193*(2), 481-493.

Gerrath JM, Lacroix CR. 1997. Heteroblastic Sequence and Leaf Development in Leea guineensis. *International Journal of Plant Sciences, 158*(6), 747-756. doi: 10.1086/297486

Gerrath JM, Posluszny U, Dengler NG. 2001. Primary vascular patterns in the Vitaceae. *International Journal of Plant Sciences, 162*(4), 729-745.

Gerrath JM, Posluszny U, Melville L. 2015. *Taming the wild grape: botany and horticulture in the Vitaceae*. Springer.

Gerrath JM, Wilson T, Posluszny U. 2004. Morphological and anatomical development in the Vitaceae. VII. Floral development in *Rhoicissus digitata* with respect to other genera in the family. *Canadian Journal of Botany, 82*(2), 198-206. doi: 10.1139/b03-120

Gray RA. 1957. Alteration of leaf size and shape and other changes caused by gibberellins in plants. *American Journal of Botany*, *44*(8), 674-682.

Grossmann K. 1990. Plant growth retardants as tools in physiological research. *Physiologia Plantarum, 78*(4), 640-648.

Gunawardena AH, Dengler NG. 2006. Alternative modes of leaf dissection in monocotyledons. *Botanical Journal of the Linnean Society, 150*(1), 25-44.

Gupta R, Chakrabarty SK. 2013. Gibberellic acid in plant: still a mystery unresolved. *Plant Signaling & Behavior*, *8*(9), e25504.

Hagemann W, Gleissberg S. 1996. Organogenetic capacity of leaves: the significance of marginal blastozones in angiosperms. *Plant Systematics and Evolution, 199*(3-4), 121-152.

Hall BG. 2013. Building phylogenetic trees from molecular data with MEGA. *Molecular Biology and Evolution, 30*(5), 1229-1235.

Hamant O, Heisler MG, Jönsson H, Krupinski P, Uyttewaal M, Bokov P, Couder Y. 2008. Developmental patterning by mechanical signals in Arabidopsis. *Science, 322*(5908), 1650-1655.

Hay A, Tsiantis M. 2006. The genetic basis for differences in leaf form between *Arabidopsis thaliana* and its wild relative *Cardamine hirsuta*. *Nature Genetics, 38*(8), 942.

Hay A, Tsiantis M. 2010. KNOX genes: versatile regulators of plant development and diversity. *Development, 137*(19), 3153-3165.

Ingrouille MJ, Chase MW, Fay MF, Bowman D, Vanderbank M, Bruijn AD. 2002. Systematics of Vitaceae from the viewpoint of plastid rbcL DNA sequence data. *Botanical Journal of the Linnean Society, 138*(4), 421-432.

Ikeda M, Ohme-Takagi M. 2014. TCPs, WUSs, and WINDs: families of transcription factors that regulate shoot meristem formation, stem cell maintenance, and somatic cell differentiation. *Frontiers in Plant Science*, 5, 427.

Initiative NGAW. 2007. The Impact of Wine, Grapes and Grape Products on the American Economy: Family Businesses Building Value.

Iwata H, Ukai Y. 2002. SHAPE: A computer program package for quantitative evaluation of biological shapes based on elliptic Fourier descriptors. *Journal of Heredity, 93*, 384-385

Jaffe MJ, Galston AW. 1968. The physiology of tendrils. *Annual Review of Plant Physiology, 19*(1), 417-434.

Jansen RK, Kaittanis C, Saski C, Lee SB, Tomkins J, Alverson AJ, Daniell H. 2006. Phylogenetic analyses of *Vitis* (Vitaceae) based on complete chloroplast genome sequences: effects of taxon sampling and phylogenetic methods on resolving relationships among rosids. *BMC Evolutionary Biology, 6*(1), 32.

Jenik PD, Barton MK. 2005. Surge and destroy: the role of auxin in plant embryogenesis. *Development, 132*(16), 3577-3585.

Jones A, Doughan B, Gerrath J, Kang J. 2013. Development of leaf shape in two North American native species of *Ampelopsis* (Vitaceae). *Botany, 91*(12), 857-865. doi:10.1139/cjb-2013-0210

Jones CS. 1999. An essay on juvenility, phase change, and heteroblasty in seed plants. *International Journal of Plant Sciences, 160*(S6), S105-S111.

Joo JH, Bae YS, Lee JS. 2001. Role of auxin-induced reactive oxygen species in root gravitropism. *Plant Physiology, 126*(3), 1055-1060.

Kim M, Pham T, Hamidi A, McCormick S, Kuzoff RK, Sinha N. 2003. Reduced leaf complexity in tomato wiry mutants suggests a role for PHAN and KNOX genes in generating compound leaves. *Development, 130*(18), 4405-4415.

Klein LL, Caito M, Chapnick C, Kitchen C, O'Hanlon R, Chitwood DH, Miller AJ. 2017. Digital morphometrics of two North American grapevines (*Vitis*: Vitaceae) quantifies leaf variation between species, within species, and among individuals. *Frontiers in Plant Science, 8*, 373.

Koyama T, Mitsuda N, Seki M, Shinozaki K, Ohme-Takagi M. 2010. TCP transcription factors regulate the activities of ASYMMETRIC LEAVES1 and miR164, as well as the auxin response, during differentiation of leaves in Arabidopsis. *The Plant Cell, 22*(11), 3574-3588.

Koyama T, Sato F, Ohme-Takagi M. 2017. Roles of miR319 and TCP transcription factors in leaf development. *Plant Physiology*, pp-00732.

Kuhl FP, Giardina CR. 1982. Elliptic Fourier features of a closed contour. *Comp Graphics Image Processing, 18*, 236-258.

Lacroix CR, Gerrath JM, Posluszny U. 1990. The Developmental Morphology of *Leea guineensis*. I. Vegetative Development. *Botanical Gazette, 151*(2), 204-209.

Leung J, Giraudat J. 1998. Abscisic acid signal transduction. *Annual Review of Plant Biology, 49*(1), 199-222.

Lincoln C, Chuck G, Hake S. 1996. KNAT1 induces lobed leaves with ectopic meristems when overexpressed in Arabidopsis. *The Plant Cell, 8*(8), 1277-1289.

Lu L, Wang W, Chen Z, Wen J. 2013. Phylogeny of the non-monophyletic Cayratia Juss. (Vitaceae) and implications for character evolution and biogeography. *Molecular Phylogenetics and Evolution, 68*(3), 502-515.

Ludwig-Müller J. 2011. Auxin conjugates: their role for plant development and in the evolution of land plants. *Journal of Experimental Botany, 62*(6), 1757-1773.

Maksymowych R, Maksymowych A. 1973. Induction of Morphogenetic Changes and Acceleration of Leaf Initiation by Gibberellic Acid in *Xanthium pennsylvanicum*. *American Journal of Botany, 60*(9), 901-906.

Marth PC, Audia WV, Mitchell JW. 1956. Effects of gibberellic acid on growth and development of plants of various genera and species. *Botanical Gazette, 118*(2), 106-111.

Migicovsky Z, Li M, Chitwood DH, Myles S. 2018. Morphometrics reveals complex and heritable apple leaf shapes. *Frontiers in Plant Science, 8*, 2185.

Mueller RJ. 1982. Shoot ontogeny and the comparative development of the heteroblastic leaf series in *Lygodium japonicum* (Thunb) Sw. *Botanical Gazette, 143*(4), 424-438.

Müller KJ, He X, Fischer R, Prüfer D. 2006. Constitutive knox1 gene expression in dandelion (*Taraxacum officinale*) changes leaf morphology from simple to compound. *Planta, 224*(5), 1023-1027.

Murray JA, Jones A, Godin C, Traas J. 2012. Systems Analysis of Shoot Apical Meristem Growth and Development: Integrating Hormonal and Mechanical Signaling. *The Plant Cell, 24*(10), 3907-3919.

Nambara E, Marion-Poll A. 2005. Abscisic acid biosynthesis and catabolism. *Annu. Rev. Plant Biology, 56*, 165-185.

Nardmann J, Werr W. 2007. The evolution of plant regulatory networks: what Arabidopsis cannot say for itself. *Current Opinion in Plant Biology, 10*(6), 653-659.

Nie ZL, Sun H, Manchester SR, Meng Y, Luke Q, Wen J. 2012. Evolution of the intercontinental disjunctions in six continents in the *Ampelopsis* clade of the grape family (Vitaceae). *BMC Evolutionary Biology, 12*(1), 17.

Ninnemann H, Zeevaart JA, Kende H, Lang A. 1964. The plant growth retardant CCC as inhibitor of gibberellin biosynthesis in Fusarium moniliforme. *Planta, 61*(3), 229-235.

Ori N, Cohen AR, Etzioni A, Brand A, Yanai O, Shleizer S, Alvarez JP. 2007. Regulation of LANCEOLATE by miR319 is required for compound-leaf development in tomato. *Nature Genetics, 39*(6), 787.

Palatnik JF, Allen E, Wu X, Schommer C, Schwab R, Carrington JC, Weigel D. 2003. Control of leaf morphogenesis by microRNAs. *Nature, 425*(6955), 257.

Park PJ, Aguirre WE, Spikes DA, Miyazaki JM. 2013. Landmark-Based Geometric Morphometrics: What fish shapes can tell us about fish evolution. *Proceedings of the Association for Biology Laboratory Education, 34*, 361-371.

Pérez FJ, Gómez M. 2000. Possible role of soluble invertase in the gibberellic acid berry-sizing effect in Sultana grape. *Plant Growth Regulation, 30*(2), 111-116.

Pharis RP, King RW. 1985. Gibberellins and reproductive development in seed plants. *Annual Review of Plant Physiology, 36*(1), 517-568.

Plotze RDO, Falvo M, Pádua JG, Bernacci LC, Vieira MLC, Oliveira GCX, Bruno OM. 2005. Leaf shape analysis using the multiscale Minkowski fractal dimension, a new morphometric method: a study with Passiflora (Passifloraceae). *Canadian Journal of Botany, 83*(3), 287-301.

Poethig RS. 2013. Vegetative phase change and shoot maturation in plants. In *Current Topics in Developmental Biology, 105*, 125-152. Academic Review.

Rademacher W. 2000. Growth retardants: effects on gibberellin biosynthesis and other metabolic pathways. *Annual Review of Plant Biology, 51*(1), 501-531.

Remagnino P, Mayo S, Wilkin P, Cope J, Kirkup D. 2017. Morphometrics: A Brief Review. *Computational Botany*, 11-32. Springer, Berlin, Heidelberg.

Ridsdale CE. 1972. Leeaceae. *Flora Malesiana-Series 1, Spermatophyta, 7*(1), 755-782.

Roberts S, Everson R. 2001. Independent component analysis: principles and practice. Cambridge University Press.

Rowland SD, Zumstein K, Nakayama H, Cheng Z, Flores AM, Chitwood DH, Sinha NR. 2019. Leaf shape is a predictor of fruit quality and cultivar performance in tomato. *bioRxiv*, 584466.

Scarpella E. 2017. The logic of plant vascular patterning. Polarity, continuity and plasticity in the formation of the veins and of their networks. *Current Opinion in Genetics & Development, 45*, 34-43.

Schneider A. 1996. Grape variety identification by means of ampelographic and biometric descriptors. *Rivista di Viticoltura e di Enologia* (Italy).

Shani E, Ben-Gera H, Shleizer-Burko S, Burko Y, Weiss D, Ori N. 2010. Cytokinin regulates compound leaf development in tomato. *The Plant Cell*, tpc-110.

Sherry RA, Lord EM. 1996. Developmental stability in leaves of *Clarkia tembloriensis* (Onagraceae) as related to population outcrossing rates and heterozygosity. *Evolution, 50*(1), 80-91.

Shwartz I, Levy M, Ori N, Bar M. 2016. Hormones in tomato leaf development. *Developmental Biology, 419*(1), 132-142.

Sinnott EW. 1923. *Botany: Principles and Problems*. McGraw-Hill book Company, Incorporated.

Skriver K, Mundy J. 1990. Gene expression in response to abscisic acid and osmotic stress. *The Plant Cell, 2*(6), 503.

Soejima A, Wen J. 2006. Phylogenetic analysis of the grape family (Vitaceae) based on three chloroplast markers. *American Journal of Botany*, *93*(2), 278-287.

Sousa-Baena MS, Lohmann LG, Hernandes-Lopes J, Sinha NR. 2018. The molecular control of tendril development in angiosperms. *New Phytologist*, *218*(3), 944-958.

Sousa-Baena MS, Lohmann LG, Rossi M, Sinha NR. 2014. Acquisition and diversification of tendrilled leaves in B ignonieae (B ignoniaceae) involved changes in expression patterns of SHOOTMERISTEMLESS (STM), LEAFY/FLORICAULA (LFY/FLO), and PHANTASTICA (PHAN). *New Phytologist*, 201(3), 993-1008.

Sousa-Baena MS, Sinha NR, Hernandes-Lopes J, Lohmann LG. 2018. Convergent evolution and the diverse ontogenetic origins of tendrils in angiosperms. *Frontiers in Plant Science*, 9, 403.

Spriggs EL, Schmerler SB, Edwards EJ, Donoghue MJ. 2018. Leaf Form Evolution in *Viburnum* Parallels Variation within Individual Plants. *The American Naturalist, 191*(2), 235-249.

Srinivasan C, Mullins MG. 1978. Control of flowering in the grapevine (*Vitis vinifera* L.): formation of inflorescences in vitro by isolated tendrils. *Plant Physiology, 61*(1), 127-130.

Srinivasan C, Mullins MG. 1980. Flowering in *Vitis*: effects of genotype on cytokinin-induced conversion of tendrils into inflorescences. *Vitis, 19*(4), 293-300.

Su YH, Liu YB, Zhang XS. 2011. Auxin–cytokinin interaction regulates meristem development. *Molecular Plant, 4*(4), 616-625.

Tassie L. 2010. Vine identification–knowing what you have. Grape and Wine Research and Development Corporation. Fact Sheet, Australian Government.

Tsukaya H. 2018. Leaf shape diversity with an emphasis on leaf contour variation, developmental background, and adaptation. In *Seminars in Cell & Developmental Biology*. Academic Press.

Tsukaya H. 2004. Leaf shape: genetic controls and environmental factors. *International Journal of Developmental Biology*, *49*(5-6), 547-555.

Veron JE. 2008. Mass extinctions and ocean acidification: biological constraints on geological dilemmas. *Coral Reefs, 27*(3), 459-472.

Uchida N, Kimura S, Koenig D, Sinha N. 2009. Coordination of leaf development via regulation of KNOX1 genes. *Journal of Plant Research, 123*(1), 7-14. doi: 10.1007/s10265-009-0248-2

Wen J. 2007. Leeaceae. In *Flowering Plants· Eudicots* (pp. 221-225). Springer, Berlin, Heidelberg.

Wen J, Boggan J, Nie ZL. 2014. Synopsis of *Nekemias* Raf., a segregate genus from *Ampelopsis* Michx.(Vitaceae) disjunct between eastern/southeastern Asia and eastern North America, with ten new combinations. *PhytoKeys*, (42), 11.

Wen J, Lu LM, Nie ZL, Liu XQ, Zhang N, Ickert-Bond S, Chen Z. 2018. A new phylogenetic tribal classification of the grape family (Vitaceae). *Journal of Systematics and Evolution*.

Zeevaart JA. 1964. Effects of the growth retardant CCC on floral initiation and growth in Pharbitis nil. *Plant Physiology, 39*(3), 402.

Zhang N, Wen J, Zimmer EA. 2015. Expression patterns of AP1, FUL, FT and LEAFY orthologs in Vitaceae support the homology of tendrils and inflorescences throughout the grape family. *Journal of Systematics and Evolution, 53*(5), 469-476.

Zhao Y. 2010. Auxin biosynthesis and its role in plant development. *Annual Review of Plant Biology, 61*, 49-64.

Zotz G, Wilhelm K, Becker A. 2011. Heteroblasty—a review. *The Botanical Review, 77*(2), 109-151.

APPENDIX A

Node	*N. arborea*	*A. aconitifolia*
1	One terminal leaflet, one pair of lateral primary leaflets, rounded serrateions and leaf tips	Leaves simple, rounded serrations and leaf tips
2	One terminal leaflet, two pairs of lateral primary leaflets, rounded serrations and leaf tips. Two secondary leaflets present on the lateral leaflet pair most proximal to the stem	Leaves trifoliate, saw-toothed serrations and pointed leaf tips
3	One terminal leaflet, two pairs of lateral primary leaflets, rounded serrations and leaf tips. Two secondary leaflets present on the lateral leaflet pair most proximal to the stem	Leaves trifoliate, saw-toothed serrations and pointed leaf tips
4	One terminal leaflet with three pairs of lateral leaflets. Secondary leaves present on second pair of lateral leaflets. Second and tertiary leaflets present on most proximal pair of lateral leaflets	Leaves trifoliate, saw-toothed serrations and pointed leaf tips
5	One terminal leaflet with three pairs of lateral leaflets. Secondary leaves present on second pair of lateral leaflets. Second and tertiary leaflets present on most proximal pair of lateral leaflets	Leaves trifoliate, saw-toothed serrations and pointed leaf tips
6	One terminal leaflet with three pairs of lateral leaflets. Secondary leaves present on second pair of lateral leaflets. Second and tertiary leaflets present on most proximal pair of lateral leaflets	Leaves trifoliate, saw-toothed serrations and pointed leaf tips. Deep indents between both secondary veins
7	One terminal leaflet with three pairs of lateral leaflets. Secondary leaves present on second pair of lateral leaflets. Second and tertiary leaflets present on most proximal pair of lateral leaflets	Leaves trifoliate, saw-toothed serrations and pointed leaf tips. Deep indents between both secondary veins
8	One terminal leaflet with four pairs of lateral leaflets. Secondary leaves present on third pair of lateral leaflets. Second and tertiary leaflets present on most proximal pair of lateral leaflets	Leaves trifoliate, saw-toothed serrations and pointed leaf tips. Deep indents between both secondary veins
9	One terminal leaflet with four pairs of lateral leaflets. Secondary leaves present on third pair of lateral leaflets. Second and tertiary leaflets present on most proximal pair of lateral leaflets	Leaves pentafoliate, saw-toothed serrations and pointed leaf tips
10	One terminal leaflet with four pairs of lateral leaflets. Secondary leaves present on third pair of lateral leaflets. Second and tertiary leaflets present on most proximal pair of lateral leaflets	Leaves pentafoliate, saw-toothed serrations and pointed leaf tips
11	One terminal leaflet with four pairs of lateral leaflets. Secondary leaves present on third pair of lateral leaflets. Second and tertiary leaflets present on most proximal pair of lateral leaflets	Leaves trifoliate, saw-toothed serrations and pointed leaf tips. Deep indents between both secondary veins
12-20	One terminal leaflet with three pairs of lateral leaflets. Secondary leaflets present on the two most proximal pairs of lateral leaflets	

Appendix A1: Description of leaf shape at each node for each species. The left column contains node numbers.

APPENDIX B

Plant	Stage		P1	P2	P3	P4	P5	P6
A aconitifolia	Length	0-50 μm	51-95 μm	96-140 μm	141-215 μm	216+ μm		
	Structure	SAM	Single paddle-like primordium	Indents begin to separate terminal primary leaflet with first pair of lateral primary leaflets	Lateral leaflets elongated and clearly dissected from terminal leaflet. No serrations present yet	Serrations form along the margins of all leaflets		
N. arborea	Length	0-60 μm	61-95 μm	96-135 μm	136-240 μm	241-315 μm	316-550 μm	551+ μm
	Structure	SAM	Single paddle-like primordium	Indents begin to separate terminal primary leaflet with first pair of lateral primary leaflets	First pair of lateral leaflets elongated and clearly dissected from terminal leaflet	Second pair of lateral leaflets elongated and clearly dissected from pair above	Third pair of lateral leaflets elongated and clearly dissected from the pair above. Secondary leaflets also begin to form here.	Fourth pair of lateral leaflets elongated and clearly dissected from the pair above.

Appendix B1: Descriptions of leaf primordia at each stage of development for each species.

APPENDIX C

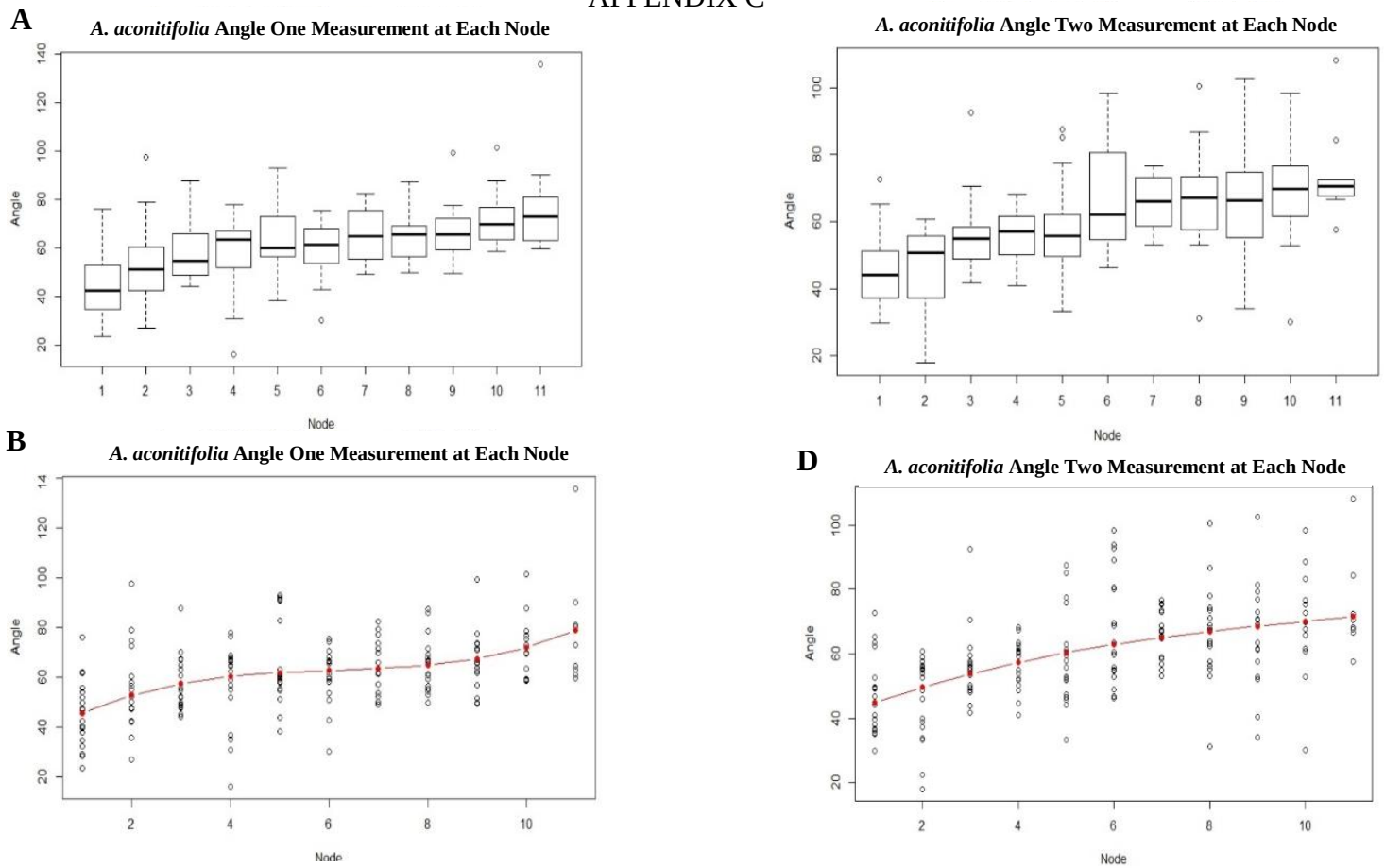

Appendix C1: *A. aconitifolia* angle one and angle two measurements at each node. (A) A boxplot showing the angle one measurements at each node along *A. aconitifolia* vines. (B) A scatterplot showing the angle one measurement at each node along *A. aconitifolia* vines with a regression line portraying the trend of the data shown in red ($p<0.0001$). (C) A boxplot showing the angle two measurements at each node along *A. aconitifolia* vines. (D) A scatterplot showing the angle two measurement at each node along *A. aconitifolia* vines with a regression line portraying the trend of the data shown in red ($p<0.0001$).

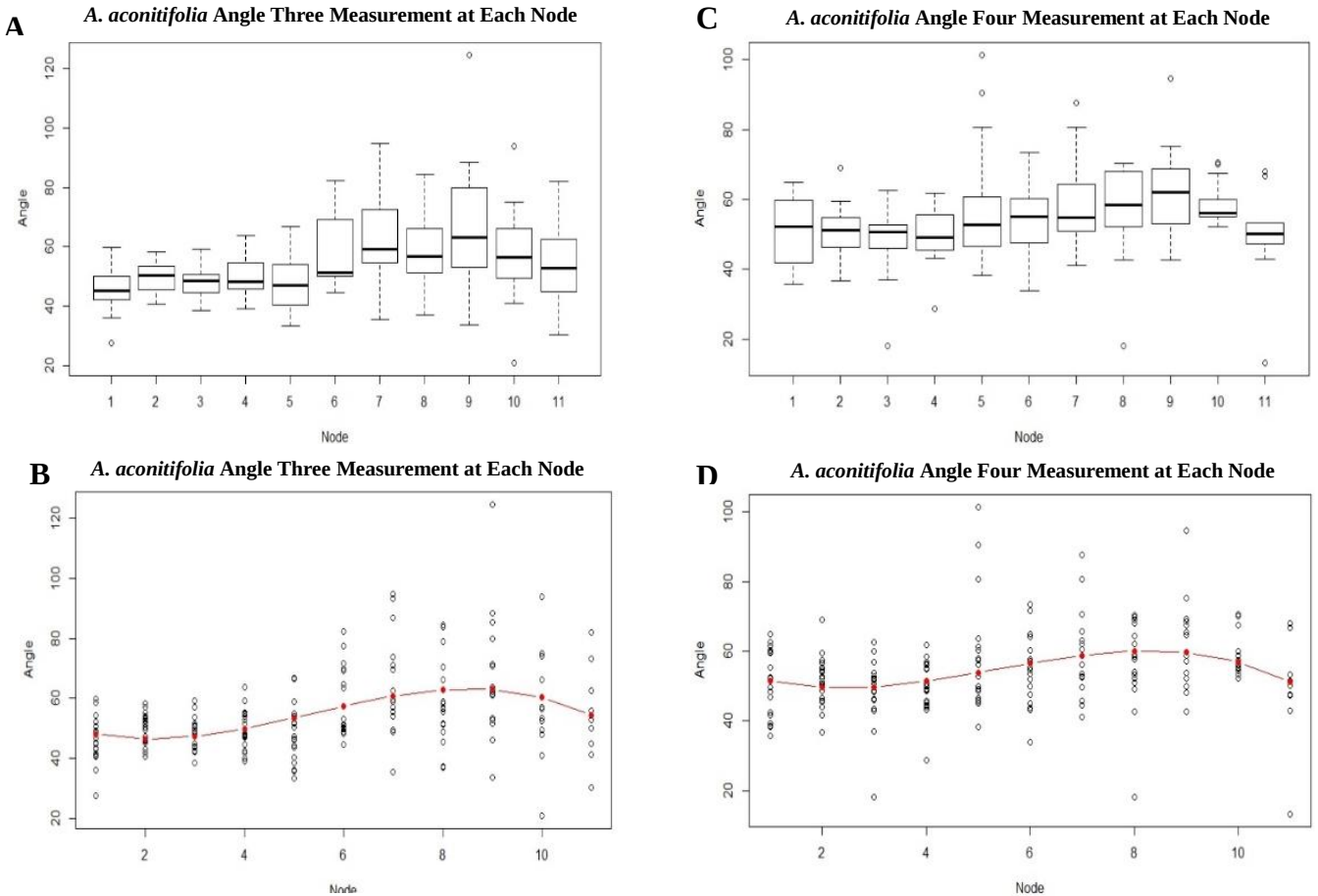

Appendix C2: *A. aconitifolia* angle three and angle four measurements at each node. (A) A boxplot showing the angle three measurements at each node along *A. aconitifolia* vines. (B) A scatterplot showing the angle three measurement at each node along *A. aconitifolia* vines with a regression line portraying the trend of the data shown in red ($p<0.0001$). (C) A boxplot showing the angle four measurements at each node along *A. aconitifolia* vines. (D) A scatterplot showing the angle four measurement at each node along *A. aconitifolia* vines with a regression line portraying the trend of the data shown in red ($p<0.0001$).

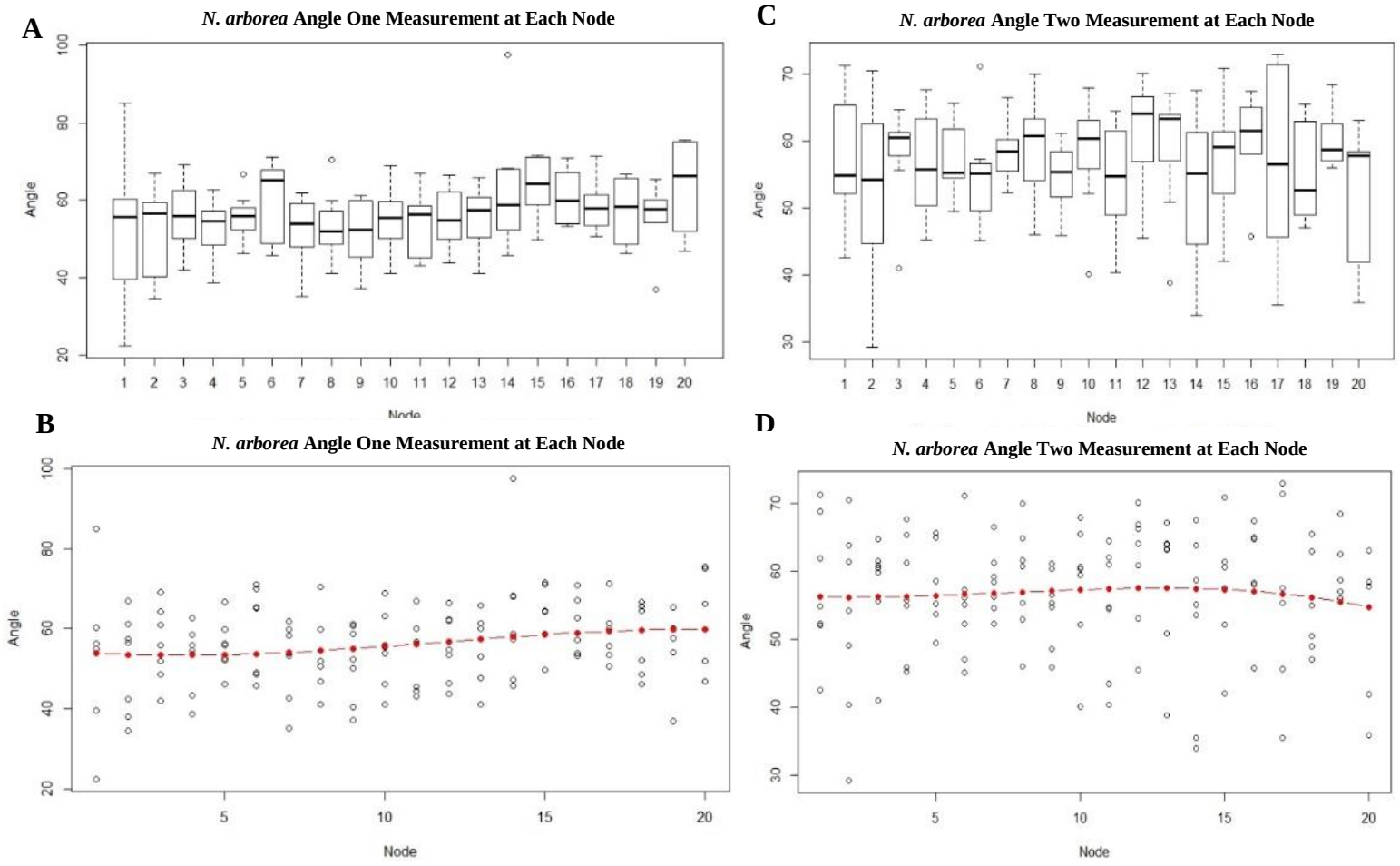

Appendix C3: *N. arborea* angle one and angle two measurements at each node. (A) A boxplot showing the angle one measurement at each node along *N. arborea* vines. (B) A scatterplot showing the angle one measurement at each node along *N. arborea* vines with a regression line portraying the trend of the data is shown in red (p=0.0389). (C) A boxplot showing the angle two measurements at each node along *N. arborea* vines. (D) A scatterplot showing the angle two measurements at each node along *N. arborea* vines with a regression line portraying the trend of the data shown in red (p=0.7886).

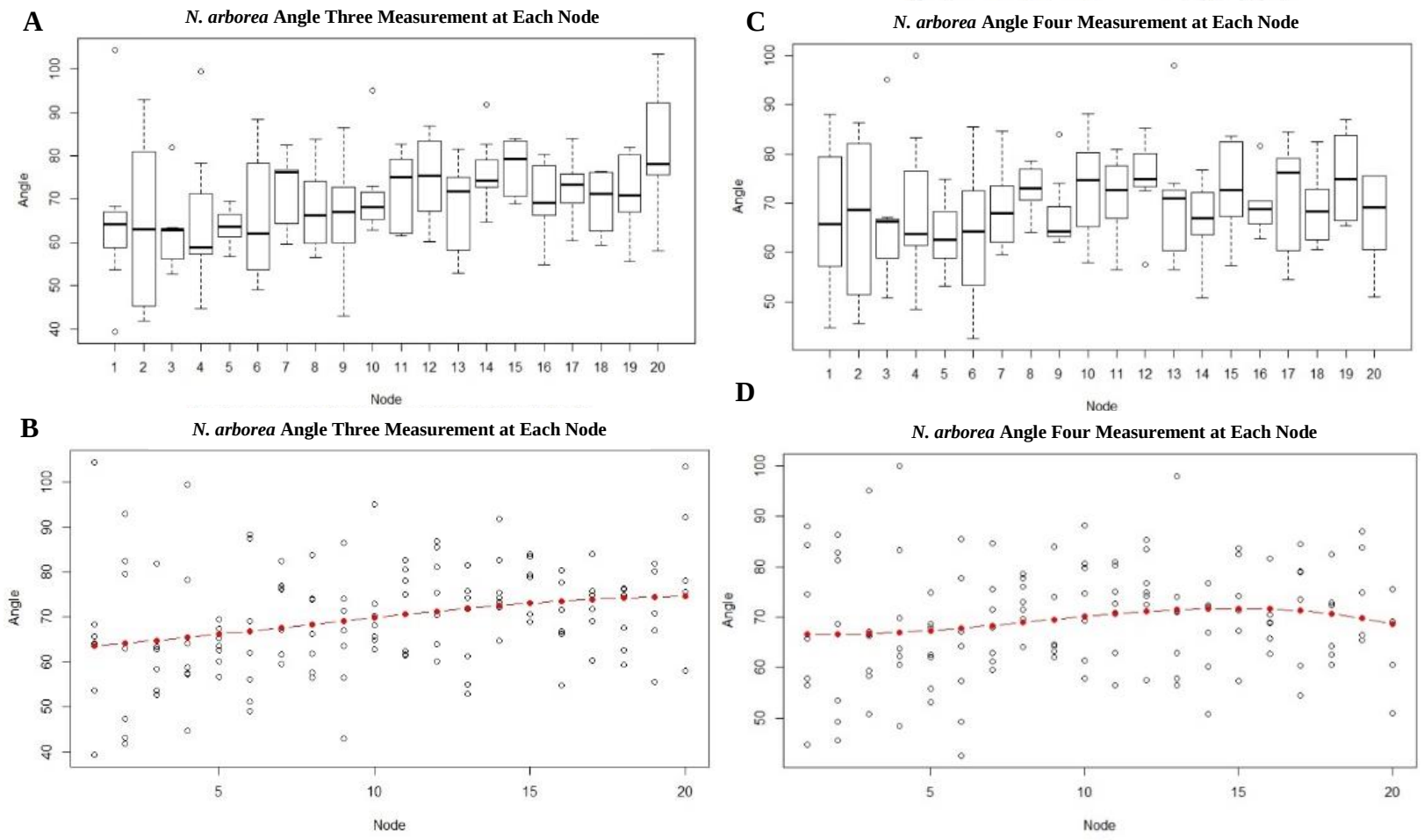

Appendix C4: *N. arborea* angle three and angle four measurements at each node. (A) A boxplot showing the angle three measurement at each node along *N. arborea* vines. (B) A scatterplot showing the angle three measurement at each node along *N. arborea* vines with a regression line portraying the trend of the data shown in red (p=0.0057). (C) A boxplot showing the angle four measurement at each node along *N. arborea* vines. (D) A scatterplot showing the angle four measurement at each node along *N. arborea* vines with a regression line portraying the trend of the data shown in red (p=0.2516).

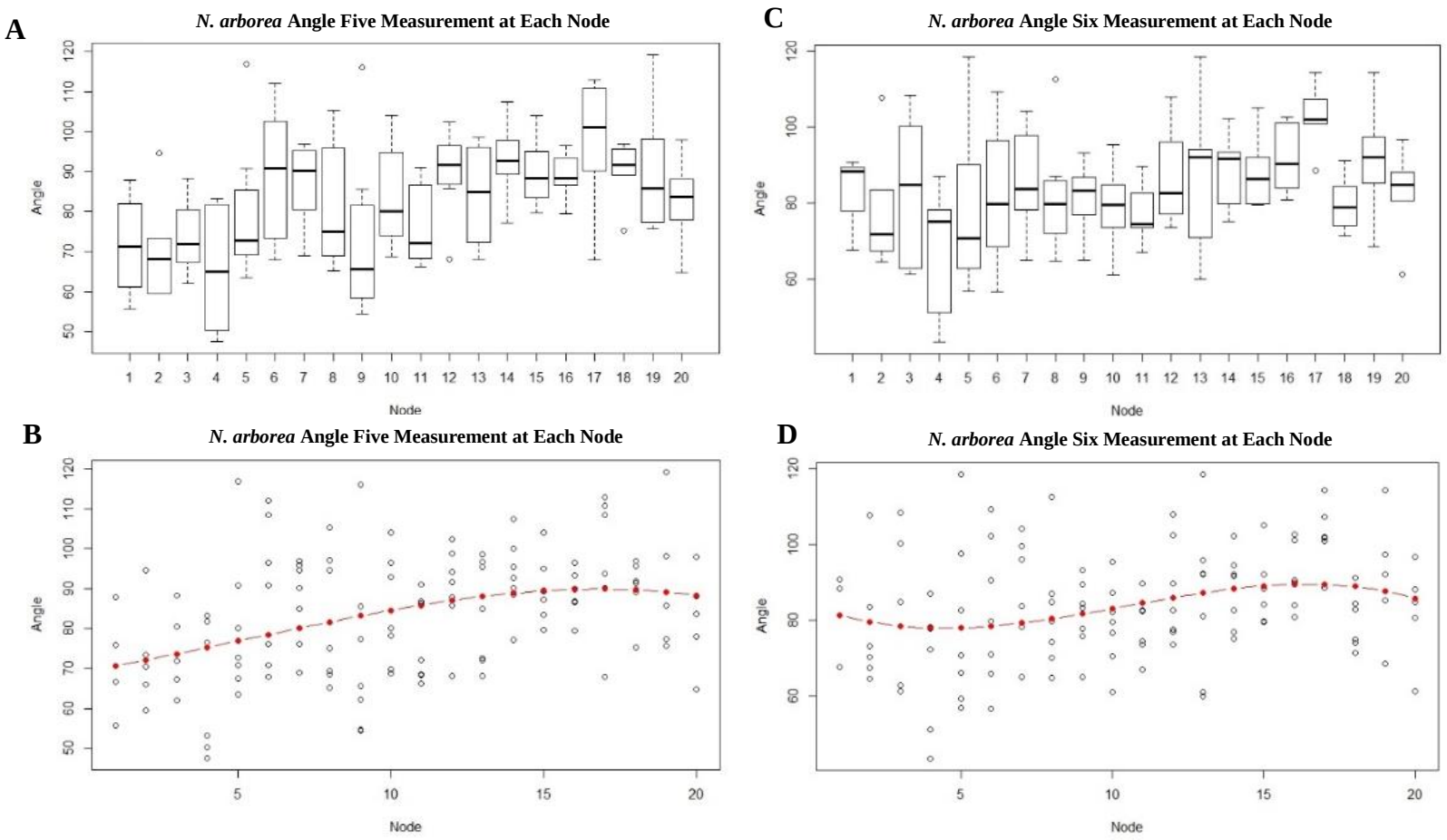

Appendix C5: *N. arborea* leaf showing the angle five measurement angle five and angle six measurement at each node. (A) A boxplot showing the angle five measurements at each node along *N. arborea* vines. (B) A scatterplot showing the angle five measurements at each node along *N. arborea* vines with a regression line portraying the trend of the data shown in red (p=0.0001). (C) A boxplot showing the angle six measurement at each node along *N. arborea* vines. (D) A scatterplot showing the angle six measurement at each node along *N. arborea* vines with a regression line portraying the trend of the data shown in red (p=0.0232).

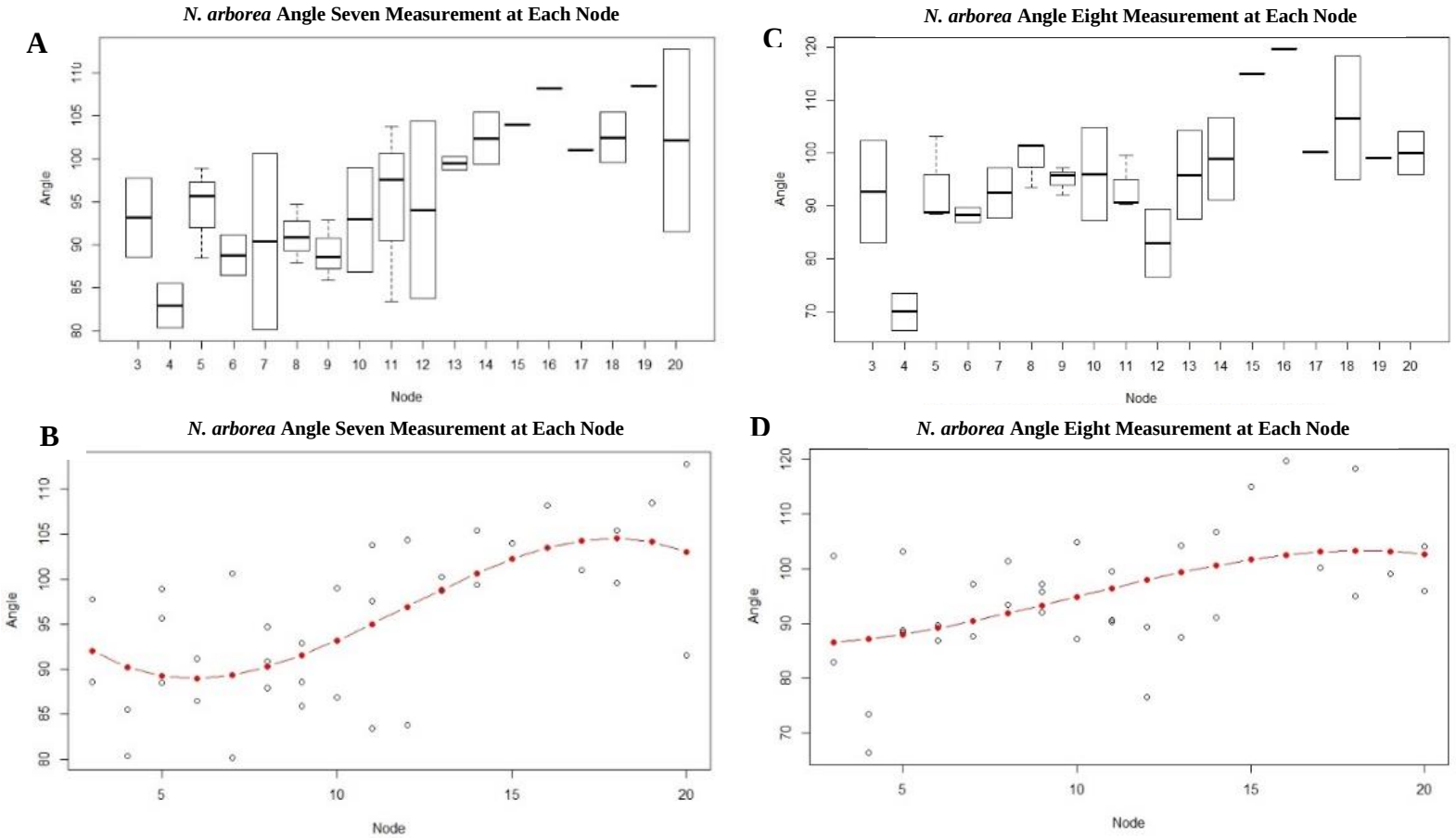

Appendix C6: *N. arborea* angle seven and angle eight measurement at each node. (A) A boxplot showing the angle seven measurements at each node along *N. arborea* vines. (B) A scatterplot showing the angle seven measurements at each node along *N. arborea* vines with a regression line portraying the trend of the data shown in red (p=0.0001). (C) A boxplot showing the angle eight measurements at each node along *N. arborea* vines. (D) A scatterplot showing the angle eight measurements at each node along *N. arborea* vines with a regression line portraying the trend of the data shown in red (p=0.0187).

APPENDIX D

Aconitifolia R Code

```
setwd("C:\\Users\\grays\\Desktop\\R Files")
.libPaths("C:\\Users\\grays\\Desktop\\R Files")
install.packages("nlme")
library(nlme)
mydata<-read.csv("AconitifoliaRData.csv")
```

Area

```
AIC(lme(Area~Node, random=~1|PlantID/Vine, data=mydata, na.action=na.exclude))
AIC(lme(Area~poly(Node, 2), random=~1|PlantID/Vine, data=mydata,
na.action=na.exclude))
AIC(lme(Area~poly(Node, 3), random=~1|PlantID/Vine, data=mydata,
na.action=na.exclude))


anova(lme(Area~poly(Node, 3), random=~1|PlantID/Vine, data=mydata,
na.action=na.exclude))
residuals(lme(Area~poly(Node, 3), random=~1|PlantID/Vine, data=mydata,
na.action=na.exclude))
hist(residuals(lme(Area~poly(Node, 3), random=~1|PlantID/Vine, data=mydata,
na.action=na.exclude)))
qqnorm(residuals(lme(Area~poly(Node, 3), random=~1|PlantID/Vine, data=mydata,
na.action=na.exclude)))
boxplot(Area~Node, data=mydata, main="A. aconitifolia Leaf Area at Each Node",
xlab="Node", ylab="Area (sq. cm)", na.action=na.exclude)
plot(Area~Node, data=mydata, main="A. aconitifolia Leaf Area at Each Node",
xlab="Node", ylab="Area (sq. cm)", na.action=na.exclude)
plot(Area~Node, data=mydata, main="A. aconitifolia Leaf Area at Each Node")
attach(mydata)
fit1<-lm(Area~poly(Node, 3), data=mydata)
points(Node, fitted(fit1), col='red', pch=20)
lines(sort(Node), fitted(fit1) [order(Node)], col='red', type='b')
```

Appendix D1: *A. aconitifolia* R code used to create p-values and graphs. The code above was used for the Area variable. Code for all other measurements were created using the same code, substituting the name of the variable wherever ‘Area’ appears in the code shown.

Arborea R Code

```
setwd("C:\\Users\\grays\\Desktop\\R Files")
.libPaths("C:\\Users\\grays\\Desktop\\R Files")
install.packages("nlme")
library(nlme)
mydata<-read.csv("Arborea R Data.csv")
```

Area

```
AIC(lme(Area~Node, random=~1|PlantID/Vine, data=mydata, na.action=na.exclude))
AIC(lme(Area~poly(Node, 2), random=~1|PlantID/Vine, data=mydata,
na.action=na.exclude))
AIC(lme(Area~poly(Node, 3), random=~1|PlantID/Vine, data=mydata,
na.action=na.exclude))


anova(lme(Area~poly(Node, 3), random=~1|PlantID/Vine, data=mydata,
na.action=na.exclude))
residuals(lme(Area~poly(Node, 3), random=~1|PlantID/Vine, data=mydata,
na.action=na.exclude))
hist(residuals(lme(Area~poly(Node, 3), random=~1|PlantID/Vine, data=mydata,
na.action=na.exclude)))
qqnorm(residuals(lm(Area~poly(Node, 3), random=~1|PlantID/Vine, data=mydata,
na.action=na.exclude)))
boxplot(Area~Node, data=mydata, main="N. arborea Leaf Area at Each Node",
xlab="Node", ylab="Area (sq. cm)", na.action=na.exclude)
plot(Area~Node, data=mydata, main="N. arborea Leaf Area at Each Node",
xlab="Node", ylab="Area (sq. cm)")
attach(mydata)
fit1<-lm(Area~poly(Node, 3), data=mydata)
points(Node, fitted(fit1), col='red', pch=20)
lines(sort(Node), fitted(fit1)[order(Node)], col='red', type='b')
```

Appendix D2: *N. arborea* R code used to create p-values and graphs. The code above was used for the Area variable. Code for all other measurements were created using the same code, substituting the name of the variable wherever ‘Area’ appears in the code shown.

APPENDIX E

	P 1	P2 V1	P2 V2	P2 V3	P3 V1	P3 V2	P4 V1	P4 V2	P5 V1	P5 V2	P5 V3	P6 V1	P6 V2	P 7	P 8	P 9	P 10	P 11	P 12
1																			
2																			
3	●	●	●	●				●	●	●	●	●			●	●		●	
4	●	●	●	●	●	●	●	●	●	●	●	●	●	●	●	●	●	●	●
5	●	●	●	●	●	●	●	●	●	●	●	●	●	●	●	●	●	●	●
6	●	●	●	●	●	●	●	●	●	●	●	●	●	●	●	●	●	●	●
7	●		●	●	●	●	●	●	●	●		●	●	●	●	●	●	●	●
8			●		●	●	●	●	●	●		●	●	●				●	●
9					●	●	●	●	●	●		●	●					●	
10					●	●	●	●	●	●		●	●					●	
11					●		●	●	●				●					●	
12													●						
13																			

Appendix E1: *A. aconitifolia* pattern of tendril initiation. Tendril pattern with node number in the left column and plant number on the top row. Dots represent tendril presence while blank squares represent tendril absence. Shaded squares mean that the vine never grew to that node length.

	Plant 1 Vine 1	Plant 1 Vine 2	Plant 1 Vine 3	Plant 2 Vine 1	Plant 2 Vine 2	Plant 2 Vine 3	Plant 3
1							
2							
3							
4							
5	●						
6	●						
7		●	●				
8	●	●	●	●	●		●
9	●			●	●	●	●
10		●	●			●	
11	●	●	●	●	●		●
12	●			●	●	●	●
13		●	●			●	
14	●	●	●	●	●		●
15	●			●	●	●	●
16		●	●			●	
17	●	●	o	o	o		●
18	●			o	o	o	o
19		o	o			o	
20	o	o	o	o			o
21	o			o			o
22		o	o				
23	o	o					
24	o						
25							
26	o						
27	o						
28							
29	o						
30	o						

Appendix E2: *N. arborea* pattern of tendril initiation. Tendril pattern with node number in the left column and plant number on the top row. Dots represent tendril presence while blank squares represent tendril absence. Open circles represent inflorescence presence. Shaded squares mean that the vine never grew to that node length.

APPENDIX F

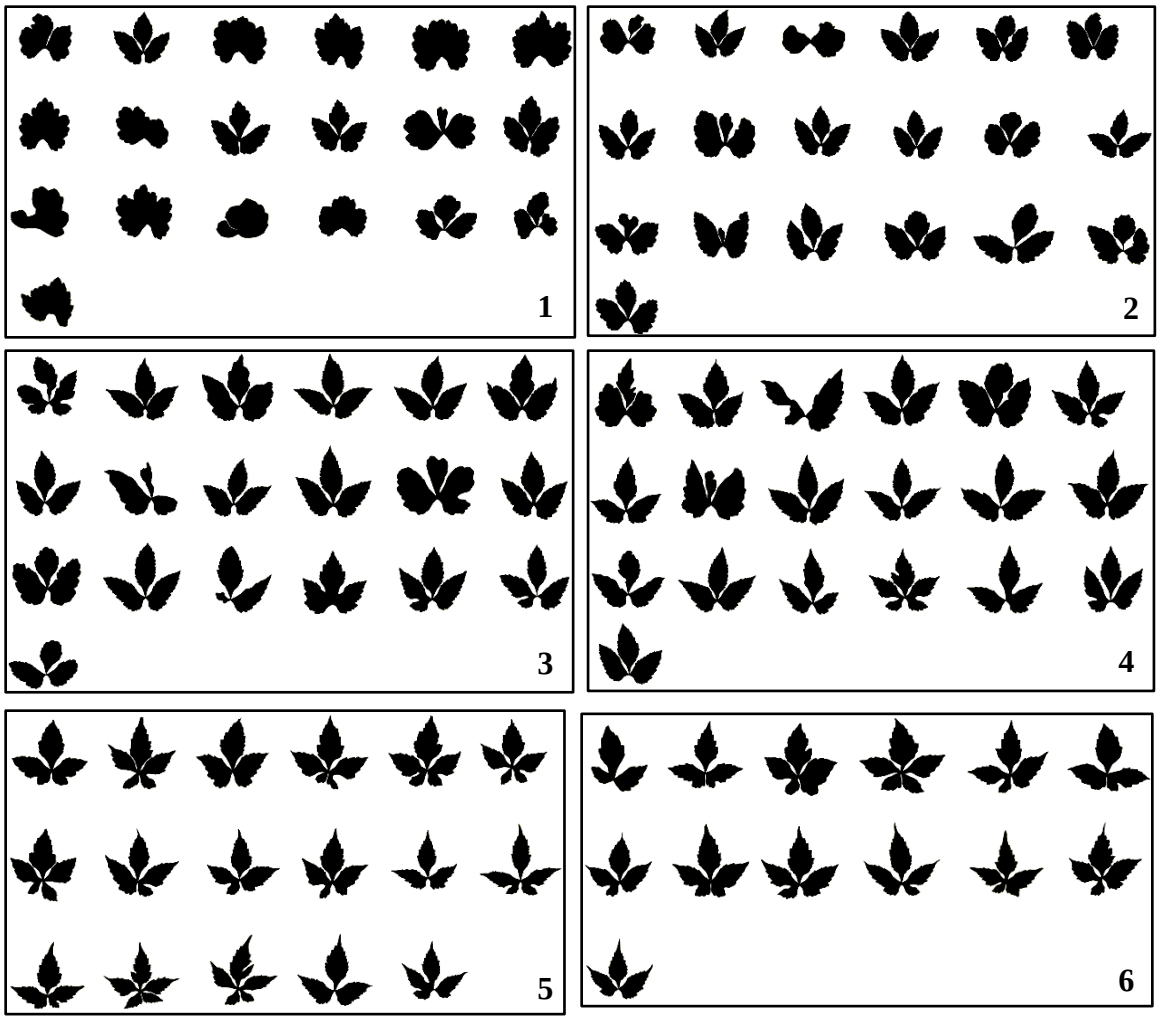

Appendix F1: *A. aconitifolia* bitmap plates showing leaf shape at each node. Numbers represent the node that all leaves found in that box were taken from.

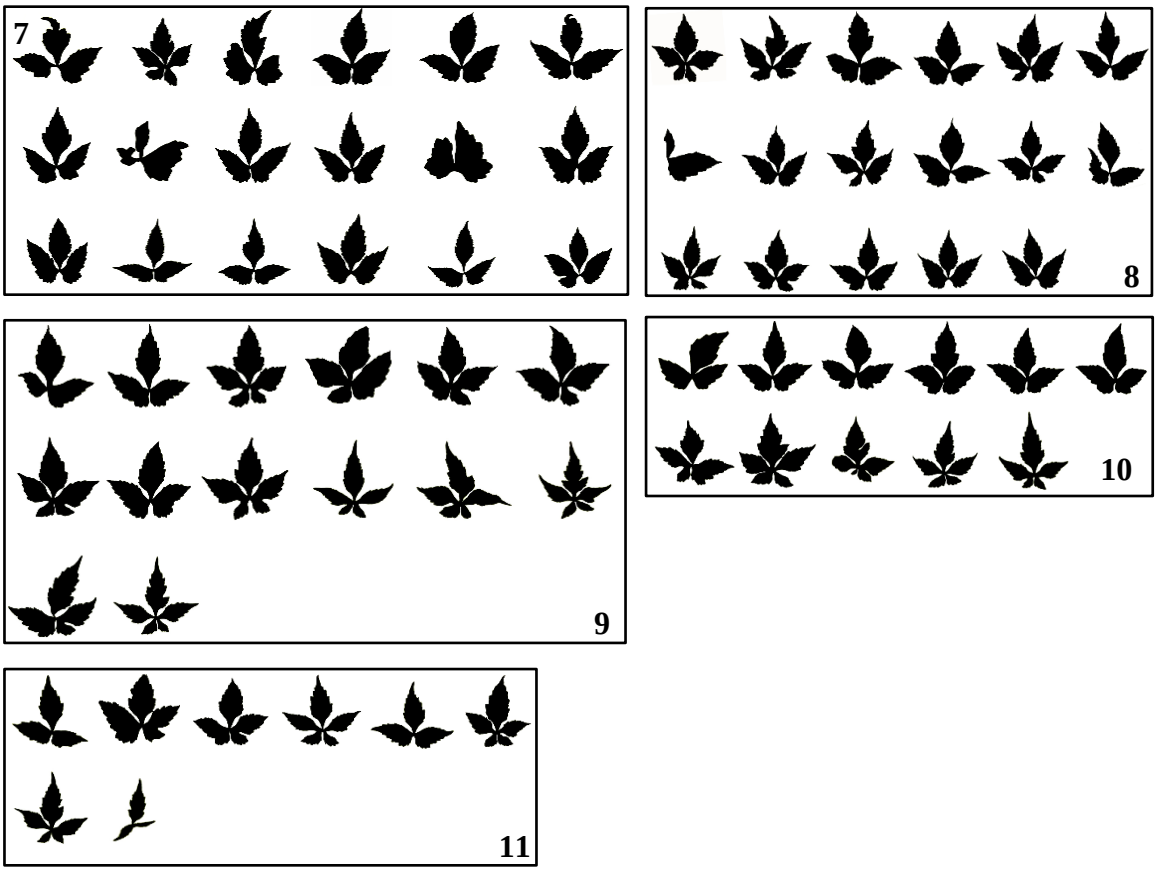

Appendix F2: *A. aconitifolia* bitmap plates showing leaf shape at each node. Numbers represent the node that all leaves found in that box were taken from.

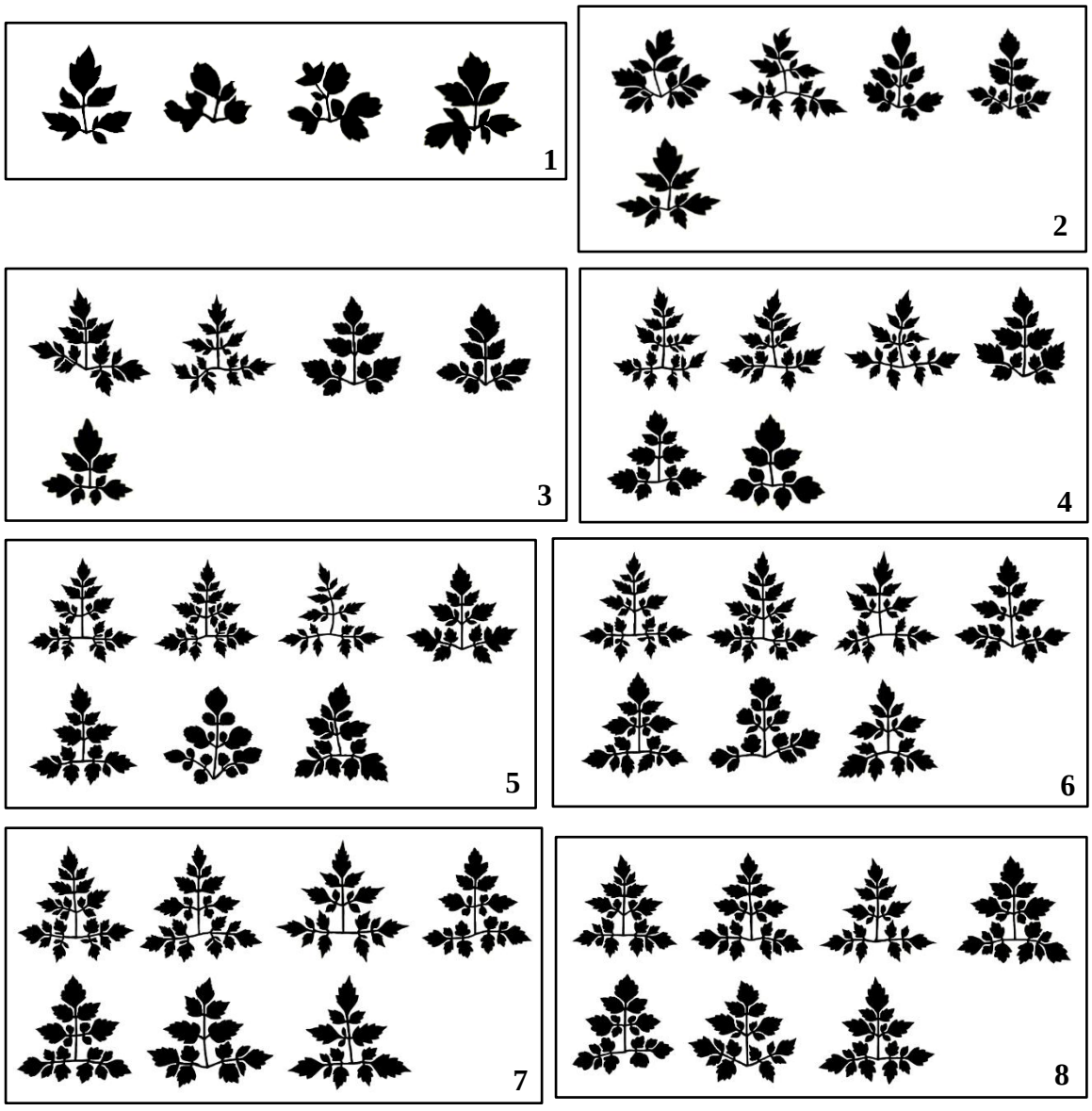

Appendix F3: *N. arborea* bitmap plates showing leaf shape at each node. Numbers represent the node that all leaves found in that box were taken from.

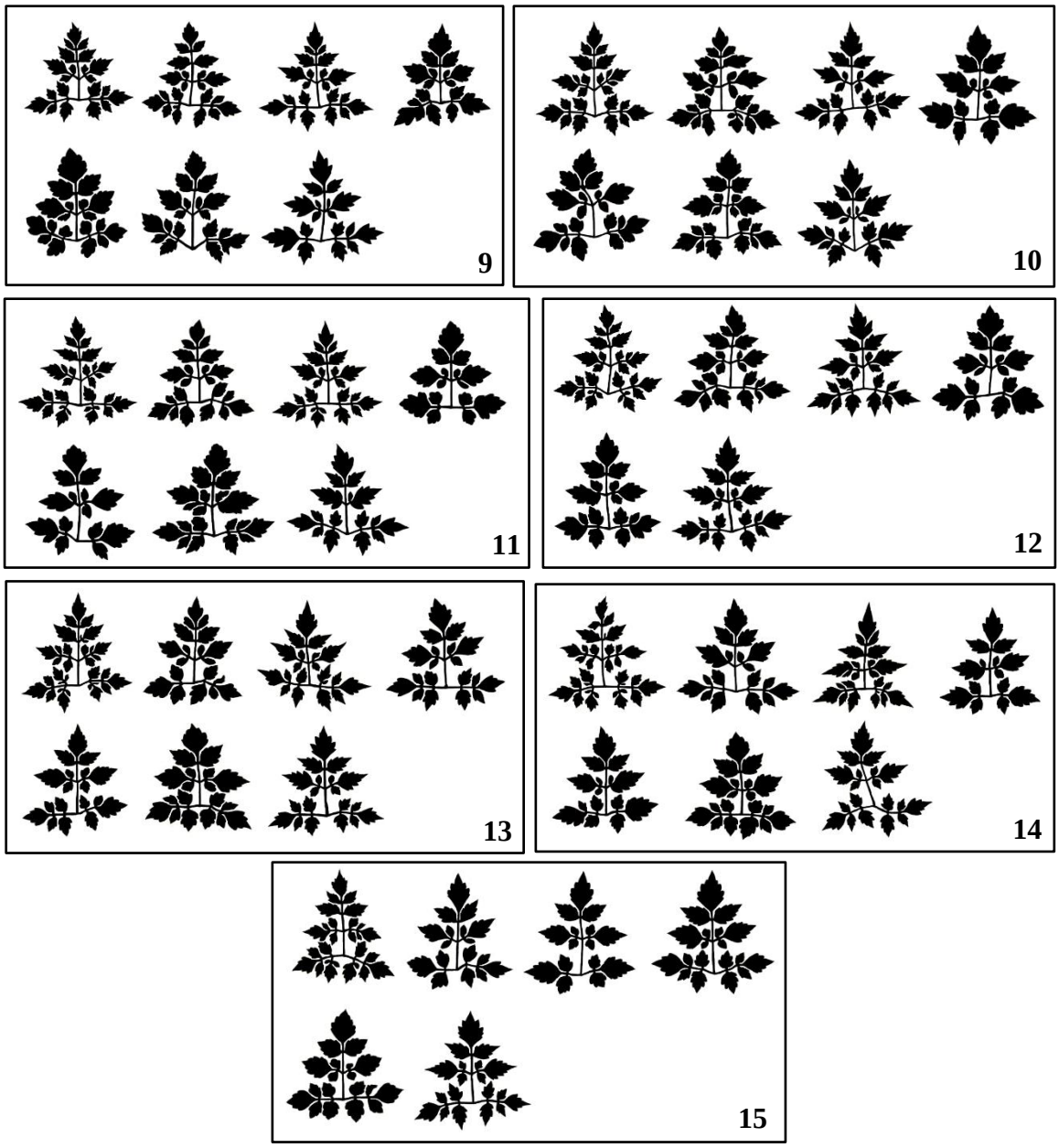

Appendix F4: *N. arborea* bitmap plates showing leaf shape at each node. Numbers represent the node that all leaves found in that box were taken from.

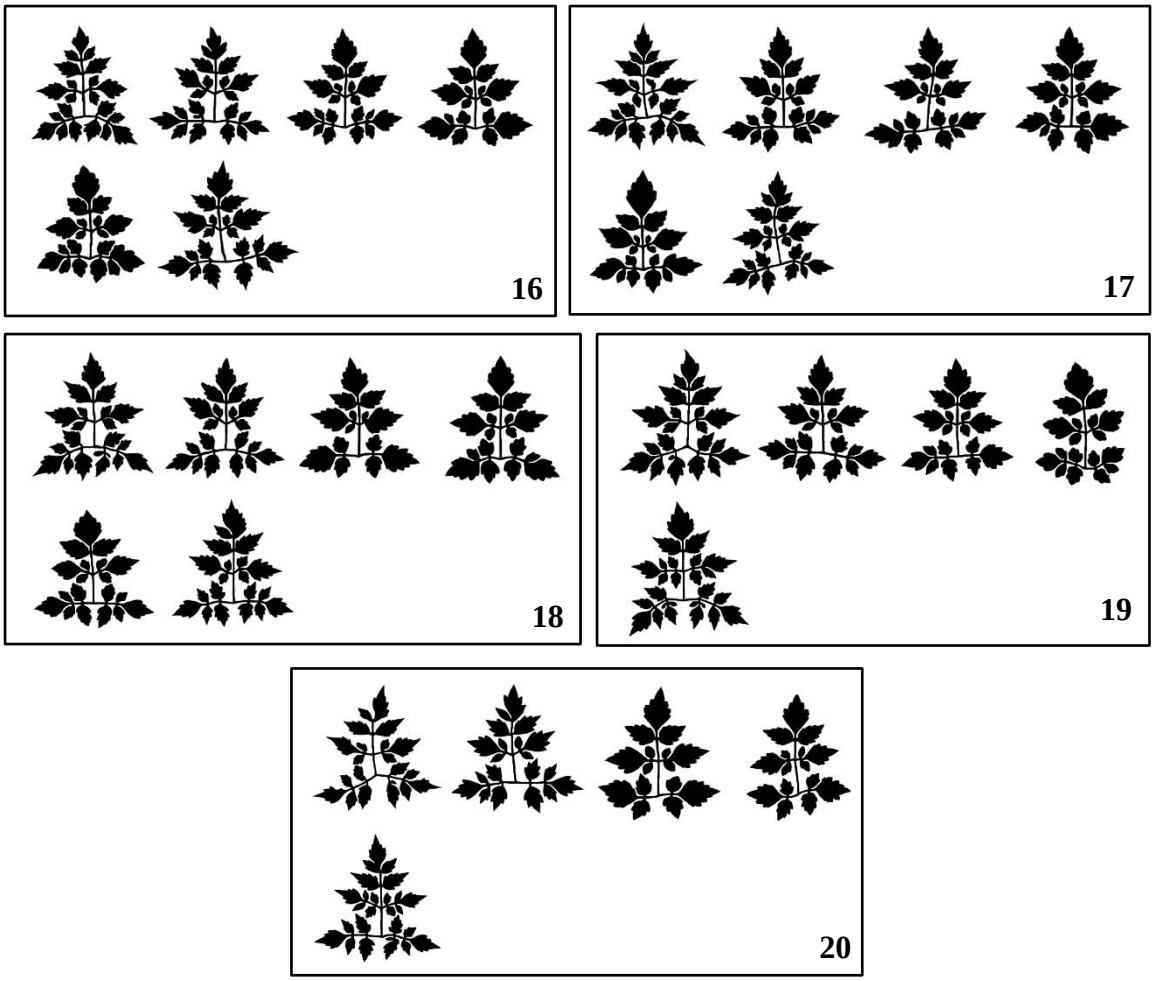

Appendix F5: *N. arborea* bitmap plates showing leaf shape at each node. Numbers represent the node that all leaves found in that box were taken from.